

**Synergistic Overview and Perspectives of 2-D Heterostructures for Cathodes  
and Separators in Flexible Li-S Batteries**

**Maryam Sadat Kiai<sup>1\*</sup>, Srikanth Ponnada<sup>2\*</sup>, Mubashir Mansoor<sup>3,4</sup>, Navid Aslfattahi<sup>5</sup>,  
Susmita Naskar<sup>6</sup>**

<sup>1</sup> Center for BioNano Interactions, School of Chemistry, University College of Dublin, Belfield, D04 C1P1 Dublin 4, Ireland

<sup>2</sup>Sustainable Materials and Catalysis Research Laboratory (SMCRL), Department of Chemistry, Indian Institute of Technology Jodhpur, Karwad, Jodhpur-342037, India

<sup>3</sup>Metallurgical and Materials Engineering Department, Istanbul Technical University, 34469 Istanbul, Turkey

<sup>4</sup>Department of Applied Physics, Istanbul Technical University, 34469 Istanbul, Turkey

<sup>5</sup>Department of Fluid Mechanics & Thermodynamics, Faculty of Mechanical engineering, Czech Technical University in Prague, Technicka' 4, 166 07, Prague, Czech Republic

<sup>6</sup>Faculty of Engineering and Physical Sciences, University of Southampton, SO17 1BJ Southampton, UK

\*Corresponding authors: maryamskiai@gmail.com; maryam.kiai@ucd.ie;  
koolsreekanth@gmail.com, srikanthponnada@mines.edu

## Abstract

Because of their high energy densities and specific capacities, lithium-sulfur (Li-S) batteries have recently received an extensive amount of research. The best way to boost battery performance is by altering electrode materials. The adoption of 2D materials-based heterostructures has attracted significant attention for increasing electrochemical performance and preventing the shuttle effect. Therefore, a summary of the link between the specific properties of 2D material heterostructures and electrochemical performance is required for the development of next-generation Li-S batteries. The present research focuses on the latest developments that boost the performance of Li-S batteries by using the unique features of 2D material heterostructures. This evaluation also categorizes several meticulously selected 2D materials with specific properties. Some solutions have been developed to overcome the difficulties of insulating intermediates, polysulfides shuttle, and sluggish kinetics. Superior conductivity, tunable functional groups, and exceptional flexibility are some of the most crucial elements in boosting electrochemical performance.

1  
2  
3 **1. Introduction**  
4  
5  
6

7 Traditional lithium-ion batteries are insufficient to meet the constantly increasing energy density  
8 demands due to the miniaturization and lightweight trends of various portable electronics as well  
9 as the rapid development of electric vehicles. A lithium sulfur battery with high theoretical energy  
10 density (2600 Wh kg<sup>-1</sup>), low cost, availability on earth and eco-friendly sulfur cathode is one of  
11 the most promising candidates in rechargeable energy storage devices. Even though Li-S batteries  
12 have so many emerging benefits, their commercial implementation is still limited by a multitude  
13 of obstacles. The intermediate lithium polysulfide species (Li<sub>2</sub>S<sub>n</sub> 2≤n<8) produced by redox  
14 reactions are readily soluble in electrolytes, resulting in the loss of active materials, passivation of  
15 the lithium anode, and shuttle effects.<sup>1</sup> Numerous efforts have been made to improve Li-S batteries'  
16 cycle life and discharge capacity. Novel electrode materials and suitable cell design are  
17 investigated to address all of these challenges. Candidates for the cathode should have good  
18 conductivity, a large surface area, and the ability to effectively capture soluble polysulfides to  
19 mitigate the shuttle effect.<sup>2, 3</sup> Due to their outstanding structural and electrical capabilities,  
20 numerous two-dimensional materials have been reported to serve as effective anchoring materials  
21 for Li-S batteries throughout the past few decades. Due to its large surface area, superior  
22 conductivity and functionalized surface, 2D hybrid materials have been widely researched.  
23 Common 2D materials consist of graphene and its variants, transition metal oxides,  
24 dichalcogenides, MXenes, black phosphorus, etc.<sup>4</sup>  
25  
26  
27  
28  
29  
30  
31  
32  
33  
34  
35  
36  
37  
38  
39  
40  
41  
42  
43  
44  
45  
46  
47  
48  
49  
50  
51  
52  
53  
54  
55  
56  
57  
58  
59  
60

The strong electrical conductivity and flexibility could enhance electron transfer and buffer volume growth. Lithium polysulfides maybe immobilized by the tunable functional groups and defects. The catalytic property enhances the transformation of lithium polysulfides to limit the shuttle effect. Numerous researchers investigated heterostructure engineering as a viable strategy for Li-S batteries to accelerate the redox kinetics of polysulfides and achieve high-rate performance. Heterostructures with various coupling components could improve reaction kinetics and speed up transportation. Yang et al. reported  $\text{TiO}_2$ -TiN heterostructures coated on a separator and demonstrated strong electrocatalytic ability to accelerate polysulfides conversion.<sup>5</sup> Sun et al. conducted a similar study using a  $\text{VO}_2$ -VN heterostructure based cathode in Li-S batteries.<sup>6</sup> 2D materials like functionalized graphene and MXenes have been created as a polysulfides riveting matrix. Defects and doped nitrogen atoms demonstrated improved polarity than pure graphene or MXenes and trapped polysulfides more strongly.<sup>7-9</sup>

The overall reaction of lithium sulfur battery reaction<sup>10</sup>

Overall:  $\text{S} + 16\text{Li} \rightleftharpoons 8\text{Li}_2\text{S}$  (1)

Cathode:  $\text{S} + 16\text{Li} + 16\text{e}^- \rightleftharpoons 8\text{Li}_2\text{S}$  (2)

Anode:  $\text{Li} \rightleftharpoons \text{Li} + \text{e}^-$  (3)

Furthermore, these phase transitions exhibit slow kinetics with the limiting step, which was previously unknown. As a result, the fundamental concerns of sulfur cathode may be divided into four distinct groups: 1) active material insulation; 2) intuitive solubility of intermediate products in organic electrolytes; 3) high volume change; and 4) slow kinetics during charge-discharge cycles. The electrochemical process is uncomplicated, the deposition of lithium anode is complex

and may be separated into three phases. Lithium nucleation and steady growth, as well as the creation of solid electrolyte interphase (SEI) films. When high active lithium encounters organic electrolyte, solid electrolyte interphase (SEI) films develop spontaneously and instantly on the metal lithium surface, causing electrolyte consumption and providing a barrier for lithium-ion transport the nucleation sites were randomly formed and in homogeneously distributed on the electrode surface during the first lithium deposition, resulting in uneven lithium dendrites. Following nucleation, lithium was constantly deposited on the nucleation sites, forming coarse dendrites that could breach the separator, resulting in battery failure and potentially fire as well as explosion <sup>9-12</sup>

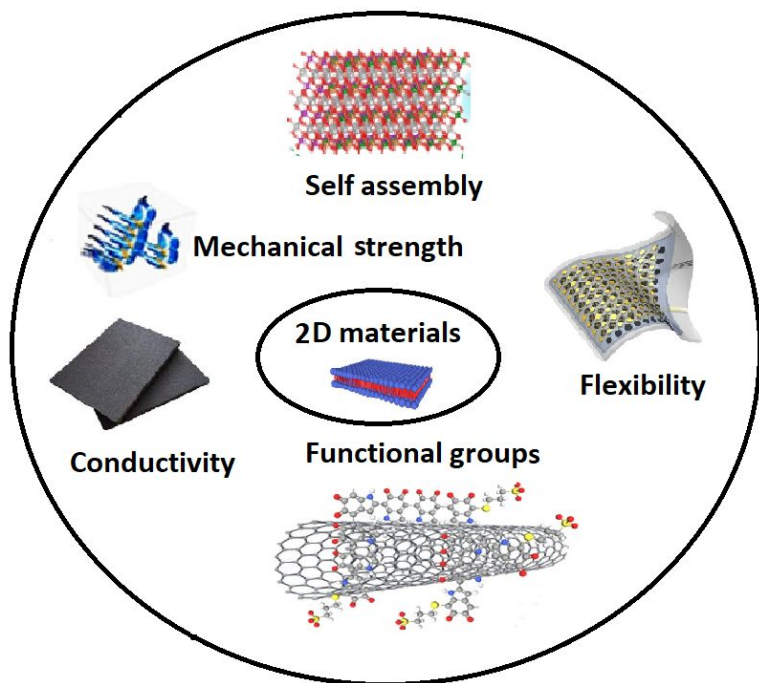
Publications on Li-S batteries have steadily grown throughout the past decade. There are considerable number of 2D hybrid materials among these. Consequently, it is required to summarize for the first time the relationship between the distinctive characteristics of 2D material heterostructures and the electrochemical performance of Li-S batteries. We presented and classified some carefully chosen 2D materials with distinct characteristics. To address the issues of insulating intermediates, polysulfides shuttle and slow kinetics, we summarized strategies for utilizing the interesting characteristics of 2D material based heterostructures such as superior conductivity, selectable functional groups and good flexibility for enhancing electrochemical performance.

This review focuses on recent advances in utilizing the unique properties of 2D material heterostructures to improve the performance of Li-S batteries. It is organized as follows: 2D materials for cathode and separator of lithium–sulfur batteries (graphene and its derivatives, transition metal oxides, dichalcogenides, MXenes and black phosphorus); DFT and mechanism

analysis for 2D materials (Heterostructures); summary and prospects for incorporating the various properties of 2D materials to promote the implementation of Li-S batteries.

## 2. Two dimensional materials for cathode and separator of lithium–sulfur batteries

Different types of 2D materials, such as graphene and its derivatives,<sup>13-17</sup> transition metal oxides (TMOs),<sup>18-20</sup> dichalcogenides (TMDs),<sup>21-23</sup> carbides and carbonitrides (MXenes),<sup>24-26</sup> black phosphorus and hexagonal boron nitride (HBN), have been investigated recently in lithium sulfur batteries. Since 2D materials are atomically stacked, they often display superior electrical, optical, and mechanical characteristics that show considerable promise for use in both basic research and practical applications.<sup>27-30</sup> In lithium-sulfur battery cathode and separator applications, 2D hybrid material electrodes demonstrated intrinsic value. The electron transfer of isolated sulfur and  $\text{Li}_2\text{S}$  was enhanced by using the high electric conductivity of 2D materials like graphene and MXenes ( $\text{Ti}_3\text{C}_2\text{X}$ ,  $\text{X} = \text{F}, \text{OH}$ ) and the abundant functional groups of hydroxyls, pyridine nitrogen, and pyrrole nitrogen on 2D materials. The most promising candidates for blocking the polysulfide shuttle effect by anchoring polysulfides in the cathode are 2D hybrid materials with high flexibility. 2D materials commonly display unique features including high electric conductivity, flexibility and mechanical strength. Moreover, the 2D materials exhibit controllable assembly feature and various functional groups. (**Schematic 1**)



**Schematic 1:** Schematic diagram of the unique properties of 2D materials for lithium sulfur batteries

**2.1. Two dimensional graphene and its derivatives**

Graphene and its derivatives are susceptible to chemical and physical interactions with sulfur and polysulfides. Graphene's geometrical features and molecular structure are responsible for the observed physical interaction. Graphene and its derivatives are flexible 2D materials that may confine sulfur particles at the macroscopic level.<sup>31</sup> Graphene and its derivatives as flexible 2D materials improve active material reutilization, reduce the shuttle effect, and protect the cathode from fracture and pulverization by trapping dissolved lithium polysulfides and buffering the significant volume change between sulfur and Li<sub>2</sub>S. Graphene exhibits a hexagonal honeycomb

crystal structure, with carbon-carbon  $sp^2$  links joining each atom and  $\pi/\pi^*$  bonds orienting off of the plane (**Fig. 1a**).<sup>32</sup>

The well-organized graphene structures successfully encapsulated the dissolute polysulfides and promoted the movement of electrons and mass. Using layered MOF templates, ultra-hydrophilic graphene stacks with very accessible nano-sized interlayer pores were manufactured. Strong static absorption of dissolved polysulfides was shown by the scaffold produced.<sup>33</sup> The synthesis of porous crumpled graphene microflowers (GmF) using spray drying and high-temperature annealing at 2000-3000<sup>0</sup> C (**Fig. 1b**)<sup>34</sup> was presented as a high-throughput production approach. In another method, caterpillar-shaped graphene was produced and sulfur was contained via a restacking process.<sup>35</sup>

Another strategy for improving the graphene/polysulfide interaction is to dope or functionalize the graphene sheet, which involves implanting heteroatoms or functional groups on the carbon's basal plane. For instance, nitrogen atoms were doped homogeneously during the CVD procedure at 750<sup>0</sup> C.<sup>36</sup> The hydroxylated, sulfureted, and fluorinated graphene nanosheets (**Fig. 1c**) were fabricated using the sonication-hydrothermal method<sup>37</sup>, intense ball milling<sup>38</sup>, and HF treatment<sup>39</sup>, which simultaneously preserved the conductivity and improved the chemical interactions, resulting in improved electrochemical performances. Doping heteroatoms onto GO sheets is another way to improve chemical bonding. Doped heteroatoms typically form chemical interactions with sulfur and lithium polysulfides. The utilization of nitrogen-doped carbon as the Li-S cathode host was investigated and several heteroatoms have been used, such as nitrogen<sup>40-42</sup>, sulfur<sup>43</sup>, phosphorus<sup>44</sup>, indium<sup>45</sup>, Fe<sup>46</sup> and boron.<sup>47,48</sup> Li NMR spectroscopy and advanced quantum chemical calculations revealed that the electron-rich donors (such as pyridinic nitrogen (pN)) are responsible for the strong dipole-dipole interaction between Li polysulfides and N-doped graphene, which is



1  
2  
3  
4  
5  
6  
7  
8  
9  
10  
11  
12  
13  
14  
15  
16  
17  
18  
19  
20  
21  
22  
23  
24  
25  
26  
27  
28  
29  
30  
31  
32  
33  
34  
35  
36  
37  
38  
39  
40  
41  
42  
43  
44  
45  
46  
47  
48  
49  
50  
51  
52  
53  
54  
55  
56  
57  
58  
59  
60

then amplified by the inductive and conjugative effect of scaffold materials with  $\pi$ -electrons (such as graphene).<sup>49-51</sup>

Moreover, Huadong Yuan et al.<sup>52</sup> demonstrated that pyridinic N atoms interact most with polysulfides (**Fig. 1d**). They also serve as active sites to reduce activation barriers for  $\text{Li}_2\text{S}$  decomposition. Even more impressive results were seen with double or triple doping.<sup>53-55</sup> By bonding S and N groups with polysulfides, a nitrogen/sulfur co-doped graphene sponge was employed as the sulfur carrier, successfully reducing the shuttle effect. Zhang et al, synthesized phosphorus codoped graphene nanosheets (P-Fe<sub>4</sub>N@NPG) using a solvothermal method and the obtained P-Fe<sub>4</sub>N@NPG/S cathode exhibited better performance in terms of polarization and shuttle effect.<sup>56</sup>

More types of functional groups or heteroatoms may be implanted, and most of the processes can be carried out at room temperature or moderate temperatures with optimized methods.

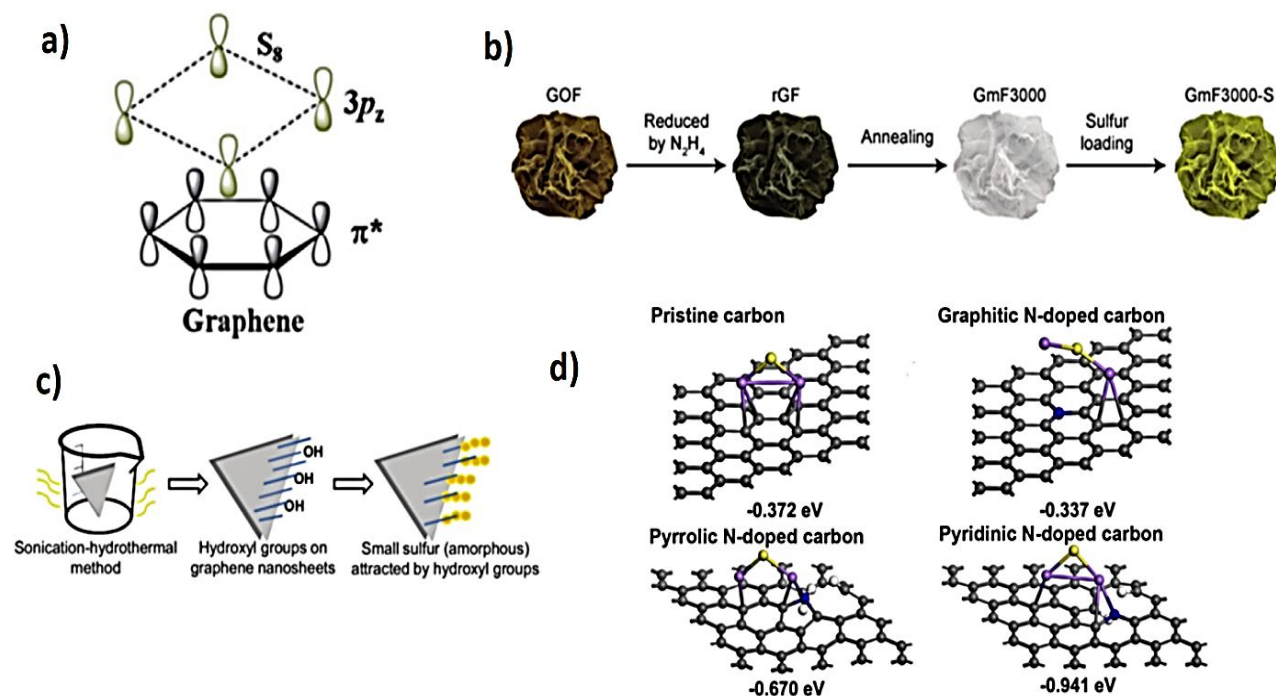


**Fig. 1** a) Both graphene and element sulfur have symmetrical, non-polar structure. Reproduced with permission from ref.32. Copyright 2013, RSC Publishing. b) Graphene microflowers produced by reducing GO at ultrahigh-temperature. Reproduced with permission from ref. 34. Copyright 2017, John Wiley and Sons. c) Hydroxylated and sulfured graphene nanosheets fabricated by sonication-hydrothermal method and intense ball milling. Reproduced with permission from ref. 37. Copyright 2013, John Wiley and Sons. d) DFT calculations of the interactions between sulfur and nitrogen atoms, showing that pyridinic N atoms have the strongest interaction with polysulfides. Reproduced with permission from ref. 52. Copyright 2018, Elsevier.

1  
2  
3 **2.2 Transition metal oxides (TMOs)**  
4

5  
6 The beneficial effects of transition metal oxide additions have been linked to strong polar  
7  
8 interactions between electron-attractive metal and negatively charged polysulfides and between  
9  
10 oxygens and Li<sup>+</sup> ions.<sup>57-60</sup> Because of their outstanding polysulfide restraining capacity, transition  
11  
12 metal oxide based on Mn and Ti has attracted special attention from the scientific community.<sup>57-</sup>  
13  
14 <sup>60</sup> Furthermore, developing sustainable sulfur composite cathodes<sup>61-63</sup> and implementing scalable  
15  
16 synthesis techniques proved to be extremely promising ways of reducing the cost-effective and  
17  
18 actually establishing a realistic Li S battery.<sup>64</sup> Recent promising work has demonstrated  
19  
20 outstanding Li S performances based on transition metal oxides with specific topologies generated  
21  
22 through alternative synthesis processes, such as three-dimensional porous MnO<sub>2</sub><sup>65</sup> and room-like  
23  
24 TiO<sub>2</sub><sup>66</sup> as sulfur hosts.  
25  
26

27  
28  
29 Hassoun et al. investigated sulfur composites with an active material weight ratio of up to 80%  
30  
31 using commercial MnO<sub>2</sub> and TiO<sub>2</sub> powders without any additional synthesis procedures.<sup>67</sup> UV-vis  
32  
33 measurements performed on the pure Li<sub>2</sub>S<sub>8</sub>-added electrolyte and on the solutions in contact with  
34  
35 MnO<sub>2</sub> and TiO<sub>2</sub> demonstrate the superior polysulfide retention of MnO<sub>2</sub>. The pure Li<sub>2</sub>S<sub>8</sub>-added  
36  
37 solution demonstrates the expected intense response, but the solution in contact with TiO<sub>2</sub>  
38  
39 produces a weaker polysulfide signal that practically disappears in the solution containing MnO<sub>2</sub>.  
40  
41

42 **(Fig. 2a)**  
43

44  
45 S MnO<sub>2</sub> has a slightly greater initial capacity than S TiO<sub>2</sub>, with 1140 and 930 mAhg<sup>-1</sup> after the  
46  
47 first cycle at 1C, respectively. However, S MnO<sub>2</sub> exhibits greater capacity deterioration throughout  
48  
49 the cycling test, with a capacity retention of 700 mAhg<sup>-1</sup> corresponding to 61% of the initial  
50  
51 capacity. At the same time, S TiO<sub>2</sub> keeps its capacity for 76% of the initial value. **(Fig. 2b).**<sup>67</sup> It  
52  
53  
54  
55  
56  
57  
58  
59  
60

suggests that nanometric  $\text{TiO}_2$  promotes faster reaction evolution than micrometric  $\text{MnO}_2$ , which may support an overload of lithium polysulfide.

Li et al. suggested Co nanoparticles embedded in N-doped CNTs.  $\text{TiO}_2$  was chosen as the skeleton due to its excellent structural and chemical durability at high voltage during charge/discharge processes. Co doping may enhance catalytic capabilities while improving conductivity.<sup>68, 69</sup> The distinctive ordered macroporous structure of Co- $\text{TiO}_2$  offers active sulfur/lithium storage interfaces. It decreases sulfur/lithium volume change during cycle, while NCNTs contribute to the porous matrix's excellent electronic conductivity and facilitate LiPS physical confinement.<sup>70</sup>

The high-resolution TEM (HRTEM) (**Fig. 2c-d**) clearly shows the carbon-coated tip Co nanoparticle with lattice spacing of 0.205 nm, corresponding to Co (111) plane. In addition, a lattice spacing of 0.324 nm was also observed, which can be assigned to  $\text{TiO}_2$  (110) plane.

DFT models proved the Li atom of LiPS likes to combine with the Co, N, and O atoms, while S prefers to coordinate with the surface Co, C, and Ti atoms. (**Fig. 2e**) The remarkable chemical adsorption performance of Co@NCNTs/Co- $\text{TiO}_2$  may commendably contribute to higher sulfur immobilization, minimizing active sulfur loss while mitigating the shuttle effect in Li-S batteries.<sup>71</sup>

Although a wide range of possible transition metal oxides can be employed<sup>72</sup>, the comprehensive study by Liang et al.<sup>73</sup>, has brought forward a general rule of thumb. They demonstrated that metal-oxides with redox potentials in the range of 2.40 V to 3.05 V are particularly effective for the inhibition of the polysulfide shuttling and thus, battery decay. Oxides that exhibit a redox potential of less than 2.4 V, such as  $\text{Co}_3\text{O}_4$  or  $\text{Ti}_4\text{O}_7$  tend to act as anchoring sites and contribute towards the polysulfide adhesion, however, they do not contribute towards conversion of polysulfides, which in itself is an important mechanism for increasing the Li-S battery lifespan. On the other hand, transition metal oxides with a redox potential of greater than 3.05 V, such as

$V_2O_5$ , tend to oxidize the polysulfide chains, forming thiosulfate/polythionate groups that are bound to the reduced metal oxide, which is not a beneficial pathway, and lead to lower cycling efficiency. The deterioration of  $MnO_2$  containing Li-S cells can be attributed to its higher limit redox potential of 3.05 V as well, which causes the unwanted oxidation of polysulfides.

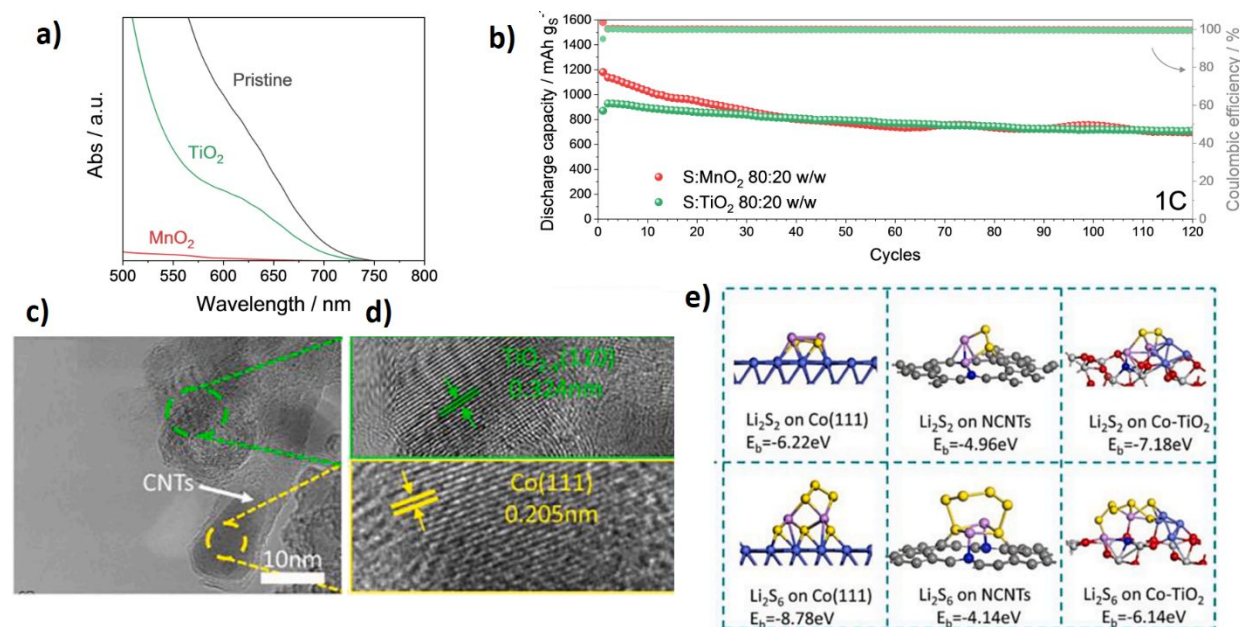


**Fig.2.** a) UV-vis measurements performed on the  $Li_2S_8$ -containing solutions in the 500–800 nm wavelength range by using a DOL: DME 1:1 w/w solution; Reproduced with permission from ref. **67**. Copyright 2023, John Wiley and Sons. b) Trends of the prolonged galvanostatic cycling tests performed on lithium cells with the configuration Li| DOL:DME, employing either S  $MnO_2$  (red) or S  $TiO_2$  (green) electrodes at a current rate of 1C; Reproduced with permission from ref. **67**. Copyright 2022, John Wiley and Sons. c, d) HRTEM images of co@ncnts/Co- $TiO_2$ ; Reproduced with permission from ref. **70**. Copyright 2013, Elsevier. e) Optimized geometries of  $Li_2S_2$  and  $Li_2S_6$  on Co (111), NCNTs and Co- $TiO_2$  surfaces. Reproduced with permission from ref. **71**. Copyright 2014, Elsevier.

He et al. proved a high tap density and excellent electrical conductivity for the obtained sulfur cathode using the transition metal oxide of  $\text{LaFeO}_3$  with perovskite structure. In addition to having exceptional electron and ion-conducting networks,  $\text{LaFeO}_3$  nanofibers made through electrospinning also appear to have outstanding chemical adsorption and catalytic activity for soluble lithium polysulfides. A high initial areal discharge capacity of  $5.9 \text{ mAh cm}^{-2}$  at high sulfur loading of  $5 \text{ mg cm}^{-2}$  has been achieved for the sulfur/ $\text{LaFeO}_3$  composite within 300 cycles at 2 C rate.<sup>74</sup> Wei et al. developed a novel macroporous Co-doped  $\text{TiO}_2$  as stable skeleton for both S and Li hosts. The achieved results exhibited a high rate capability of  $879.66 \text{ mAh g}^{-1}$  at 5C, as well as super cycling stability with a low capacity decay rate of about 0.033 % after 1000 cycles at 3C.<sup>75</sup> Pu et al. addressed the poor electrical conductivity limits of transition metal oxides through development of the homogeneous  $\text{CoNiO}_2/\text{Co}_4\text{N}$  nanowires. Strong adsorptive/catalytic properties of  $\text{CoNiO}_2$  accompanied with efficient electrical conductivity of  $\text{Co}_4\text{N}$  could significantly inhibit shuttle effect and improve the transport rate of ions and electrons.<sup>76</sup>

### 2.3. Dichalcogenides (TMDs)

Transition metal dichalcogenides (TMDs) are a prominent family of polar materials with an analogous graphene structure that have piqued the attention of academia and industry due to their unusual physical characteristics, excellent structural stability, and abundant transition metal d-electrons.<sup>77-79</sup>

Titanium disulfide ( $\text{TiS}_2$ ) has the smallest weight, lowest cost, highest stability, and best binding affinity to PS among the stacked TMDs.<sup>80-83</sup> As-obtained H- and O-incorporated porous  $\text{TiS}_2$  (HOPT) was investigated recently.<sup>82</sup> The cell design comprises a CNTsS/HOPT cathode paired with a lightweight graphene/HOPT interlayer.

The battery maintains its discharge capacity of 172 mA h g<sup>-1</sup> until the 2500th cycle, even at a current rate of 30 C, degrading at just 0.015% per cycle on average (**Fig 3a**). In addition, after 2500 cycles, the Coulombic efficiency is still more than 98%. CNTsS/ 300HOPT@G/300HOPT shows tremendous potential for long-term storage applications requiring high power output, with its high reversible capacity and low-capacity degradation rate at 30 C.

Because of the encouraging rate performance of CNTsS/300HOPT@ G/300HOPT, its high-power application is investigated. To get to 4.8 mg of S, four half-cells were built in sequence. After only 20 s of charging, the device's open circuit voltage of 9.5 V is sufficient to efficiently drive 60 white, blue, green, or red-light emitting diode (LED) indicator modules indicating CNTsS/300HOPT@G/300HOPT electrode's exceptional high-power capability. (**Fig 3b**)<sup>84</sup>

CoS<sub>2</sub>@MoS<sub>2</sub> hollow nanocages on carbon cloth (CoS<sub>2</sub>@MoS<sub>2</sub>/CC) are investigated recently and are produced by a two-step hydrothermal process. (**Fig. 3c**)<sup>85</sup>

Considering potential commercial applications, the viability of S@CoS<sub>2</sub>@MoS<sub>2</sub>/CC cathode with a greater sulfur loading is examined further. As shown in **Fig. 3d**, the cathodes with sulfur loadings of 2.0, 2.9, and 3.6 mg cm<sup>-2</sup> preserve respectable capacities of 911.8, 763.2, and 569.7 mAh g<sup>-1</sup> after 100 cycles at 0.1C. These remarkable electrochemical performances suggest that the CoS<sub>2</sub>@MoS<sub>2</sub>/CC structures may effectively improve the performance of cathodes with a high sulfur loading. **Fig.3e** depicts the cycling performance over a long period. After 300 cycles, the reversible capacities are maintained at 579.3 mAh g<sup>-1</sup> and 556.8 mAh g<sup>-1</sup>, respectively. These findings demonstrate the great stability of cycling at various current densities.<sup>85</sup>

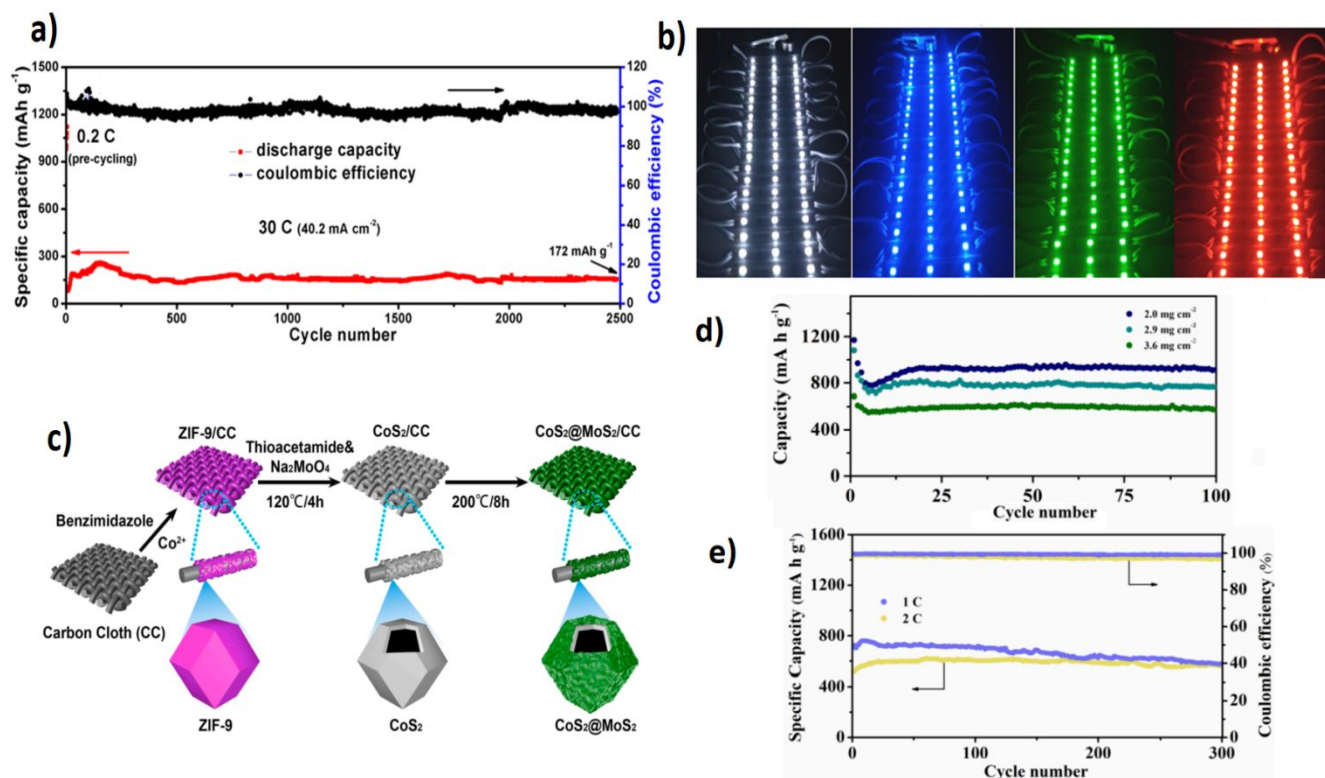


**Fig. 3** a) Cycling performance of the CNTs-S/300HOPT@G/300HOPT electrode at 30 C. Reproduced with permission from ref. **84**. Copyright 2017, American Chemical Society; b) Digital photographs of 60 white, blue, green, and red indicators composed of 2835 LED modules powered by four lithium batteries in series. Reproduced with permission from ref. **84**. Copyright 2017, American Chemical Society; c) Schematic illustrations for the fabrication of CoS<sub>2</sub>@MoS<sub>2</sub>/CC d) The cycling performance of the CoS<sub>2</sub>@MoS<sub>2</sub>/CC at 0.1C with S loading of 2.0, 2.9 and 3.6 mg cm<sup>-2</sup>; e) The long-term cycling performance of the S@CoS<sub>2</sub>@MoS<sub>2</sub>/CC at 1C and 2C, respectively. c, d, e Reproduced with permission from ref. **85**. Copyright 2022, Elsevier.

According to the latest studies, the combination of MXenes and TMDs is potentially capable of exposing the best features of both the MXenes and TMDs. Enhanced contact area between electrode and electrolyte is the result of combining MXenes and TMDs.<sup>86</sup>



Wang et al., developed a hybridized Co-MoSe<sub>2</sub>/MXene bifunctional catalyst as a high-efficient sulfur host. Authors successfully achieved a high reversible specific capacity of 1454 mAh g<sup>-1</sup> and an ultrahigh volumetric energy density of 3659 Wh L<sup>-1</sup>.<sup>87</sup>

## 2.4. MXenes

MXenes with the formula M<sub>n+1</sub>X<sub>n</sub>T<sub>x</sub> (n = 1-3) (where M represents a transition metal, X represents carbon or nitrogen, T<sub>x</sub> stands for the surface terminations). The surface of MXenes is terminated with different functional groups such as hydroxyl (OH), oxygen (O), chlorine (Cl), and fluorine (F) after etching, resulting in high hydrophilicity. The use of MXenes in Li-S batteries should be given special consideration. MXene surface groups (particularly hydroxyl groups) are extremely affinitive to polysulfides and may attract them without further surface modifications. Furthermore, the highly conductive core (Ti C Ti bonds) may considerably accelerate charge transfer kinetics, significantly improving sulfur utilization and capacity retention.<sup>88-91</sup>

Wang's team developed a crumpled nitrogen-doped Ti<sub>3</sub>C<sub>2</sub>T<sub>x</sub> (N-Ti<sub>3</sub>C<sub>2</sub>T<sub>x</sub>) nanosheet with a well-defined porosity structure to boost the affinity to sulfur. (**Fig. 4a**) Such nitrogen-doped MXenes are also more capable of adsorbing polysulfides than pure MXenes, with an improved reversible capacity of 950 mAh g<sup>-1</sup> after 200 cycles at 0.2C. (**Fig. 4b**).<sup>92</sup>

As illustrated in **Fig. 4c**, a highly conductive Mo<sub>2</sub>CT<sub>x</sub> MXene-CNT hybrid was created by interweaving with CNTs. At different sulfur loadings, the Mo<sub>2</sub>CT<sub>x</sub>/CNTs electrode showed remarkable electrochemical performances in high capacity, good rate capability, and high initial reversible capacity (1314 mAh g<sup>-1</sup> at 1.8 mg cm<sup>-2</sup> sulfur loading, 959 mAh g<sup>-1</sup> at 5.6 mg cm<sup>-2</sup> sulfur loading).<sup>93</sup> W<sub>2</sub>C has been described as an effective sulfur host with stable cycling for Li-S batteries, which might be attributed to W<sub>2</sub>C's improved adsorption and catalytic sites. Decorating W<sub>2</sub>C

nanoparticles on the CNF and loading  $W_2C$  nanoclusters on the nitrogen-phosphorous co-doped carbon matrix ( $W_2C/N/P-rGO$ ) resulted in composites with better polysulfides interaction and electrochemical kinetics (**Fig. 4d**). Under various sulfur loadings, the  $W_2C/N/P-rGO$  composite demonstrated significant reversible capabilities (**Fig. 4e**).<sup>94</sup>

MXenes could entrap the soluble  $Li_2S_n$  through a strong Ti-S interaction to inhibit the shuttling effect. Meanwhile, MXene surface functional groups exhibit robust chemisorption to  $Li_2S_n$ , effectively reducing active material loss and maintaining high capacities during long-term cycling. MXenes with certain surface groups and configurations have a low  $Li_2S$  decomposition energy barrier and rapid  $Li^+$  diffusivity, facilitating electrochemical redox processes.  $Ti_3C_2T_x$  is just one kind of MXene. More than 30 different MXene phases have been discovered so far, and their existence has been anticipated for several more. There are plenty of reasons to look at additional MXene members as a potential source for high-capacity Li-S batteries.<sup>95</sup>

Herbert and Ulam were the first to use elemental sulfur as a cathode and presented the electrochemical reaction  $2Li + S \rightleftharpoons Li_2S$  in 1962<sup>126</sup>. Rauh et al. established in 1979 that Li metal is particularly stable to highly concentrated solutions of  $Li_2S_n$  ( $n=1,2,4,6$ , and 8) in Tetrahydrofuran (THF) and other aprotic organic solvents<sup>11,95</sup>.

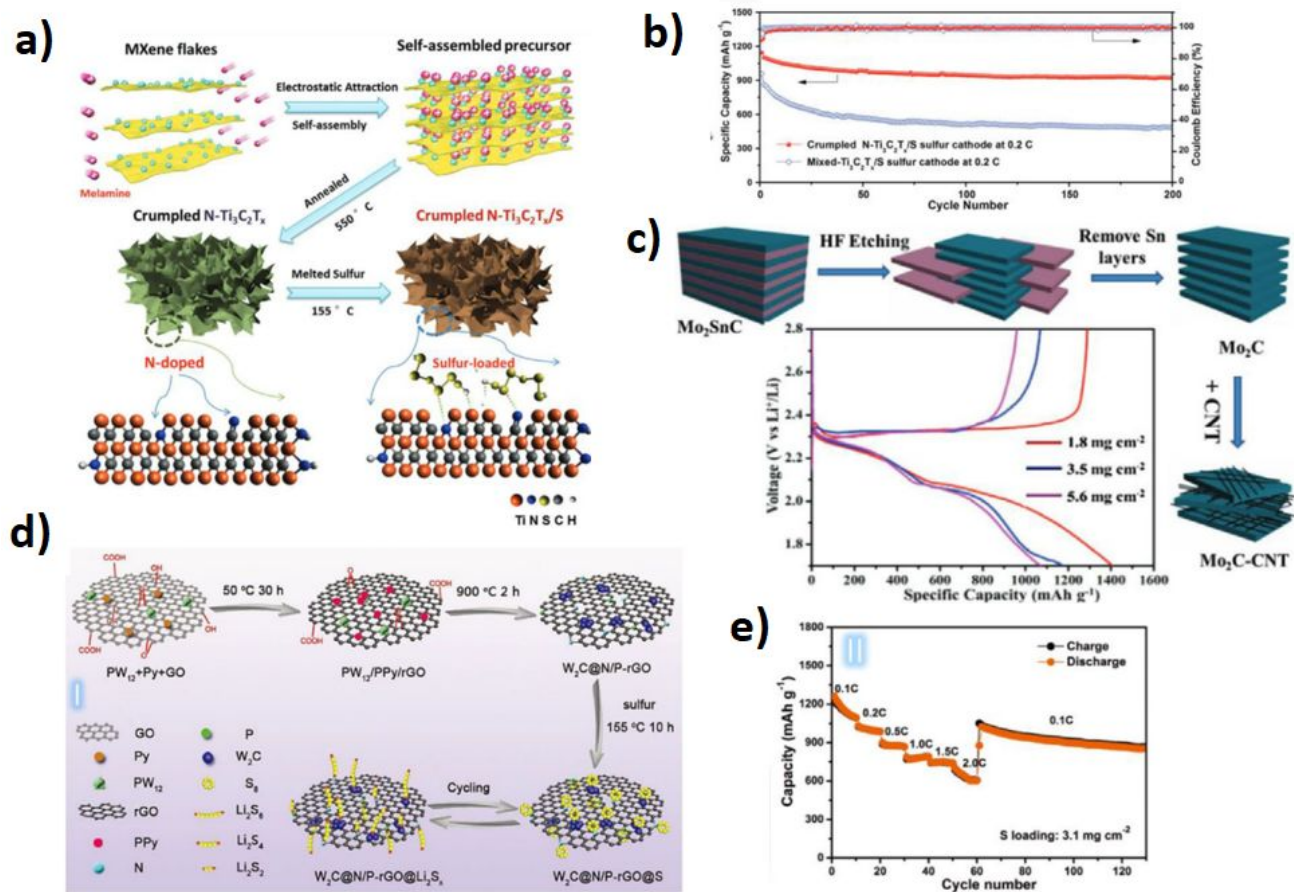


**Fig. 4.** a) Schematic illustration of synthesis process of the crumpled N-Ti<sub>3</sub>C<sub>2</sub>T<sub>x</sub>/S electrodes Reproduced with permission from ref. **92**. Copyright 2023, John Wiley and Sons; b) Cycling performances of crumpled N-Ti<sub>3</sub>C<sub>2</sub>T<sub>x</sub>/S electrode and mixed-Ti<sub>3</sub>C<sub>2</sub>T<sub>x</sub>/S electrodes. Reproduced with permission from ref. **92**. Copyright 218, John Wiley and Sons; c) Schematic diagram of the growth routine of Mo<sub>2</sub>CT<sub>x</sub>/CNT composites, and initial charging/discharging curves of Mo<sub>2</sub>CT<sub>x</sub>/CNT cells under various sulfur loadings, Reproduced with permission from ref. **2019**. Copyright 2023, John Wiley and Sons; d) Schematic illustration of the preparation strategy of W<sub>2</sub>C/N/P-rGO/S composites, Reproduced with permission from ref. **2019**. Copyright 2023, John Wiley and Sons; e) Rate ability of W<sub>2</sub>C/N/P-rGO/S cathode under different sulfur loadings. Reproduced with permission from ref. **2019**. Copyright 2023, John Wiley and Sons.

Feng et al. developed a  $\text{MoWS}_2@\text{MXene}@\text{CNT}$  composite material as the main cathode for lithium sulfur batteries. The obtained results proved a good rate and cycling stability for the investigated lithium sulfur batteries.<sup>96</sup> Zong et al. developed a  $\text{MoS}_2/\text{Nb}_2\text{C}$  catalyst as cathode with good long-term stability for Li-S batteries. Authors achieved a specific capacity of  $919.2 \text{ mAh g}^{-1}$  at  $0.2 \text{ C}$  after 200 cycles with excellent retention of 92.2%.<sup>97</sup>

## 2.5. Black phosphorus (BP)

Black phosphorus (BP) is appealing from a compositional design standpoint due to its high electrical conductivity and rapid Li-ion transport.<sup>98</sup> From an architectural standpoint, BP's two-dimensional (2D) structure reveals many edges active sites, giving LiPSs remarkable chemisorptive potential. Amorphous FeCoO-coated BP ( $\text{BP}@\text{FeCoO}$ ) nanosheets were effectively manufactured with a simple solvothermal technique.<sup>99</sup> As illustrated in **Fig. 5a**, the capacitive current in the cell with BP electrodes was insignificant. On the other hand, the symmetric cell with the  $\text{BP}@\text{FeCoO}$  electrode displayed greater peak current densities than the  $\text{BP}@\text{c-FeCoO}$  and  $\text{c-FeCoO}$  electrodes,<sup>99</sup> confirming its better catalytic activity in LiPS conversion.<sup>100-103</sup>

**Fig. 5b** depicts the good adsorption-conversion process of  $\text{BP}@\text{FeCoO}$  towards LiPSs.<sup>99</sup>

Because of its chemical interaction with LiPSs,  $\text{BP}@\text{FeCoO}$  may chemically adsorb them and provide large ion and electron conductivities, boosting LiPS conversion through fast catalytic activity.<sup>104-105</sup> The large surface area and meso/microporous architectures of  $\text{BP}@\text{FeCoO}$  reveal the abundant active sites on the surface for LiPS immobilization and allow for the volumetric expansion of sulfur.

The current theoretical work was carried out to forecast the "surface approach" via heteroatom doping of BP to improve its performance in order to lower the BP loading. Lewis acidic B-doped BP, Al-doped BP, Lewis basic N-doped BP, and virgin BP are investigated recently.

**Fig. 5c** shows the corresponding adsorption energy data for BP, N-BP, B-BP, and Al-BP. The order is as follows: B-BP > Al-BP > N-BP > BP. This implies that all N doping, B-doping, and Al-doping increase the adsorption energy value. B-BP and Al-BP adsorption energies are much higher than those of BP and N-BP. B-BP has the greatest impact on adsorption energy augmentation.<sup>106</sup> According to the calculation of  $\text{Li}_2\text{S}_2 \rightarrow \text{Li}_2\text{S}$  conversion, N-doping increases conversion energy requirements, but B-doping and Al-doping lower conversion energy requirements and improve lithium polysulfide conversion. Combining these two critical factors suggests that B and Al doping of black phosphorus is a potential "surface technique" for improving BP performance and, ultimately, lowering loading.

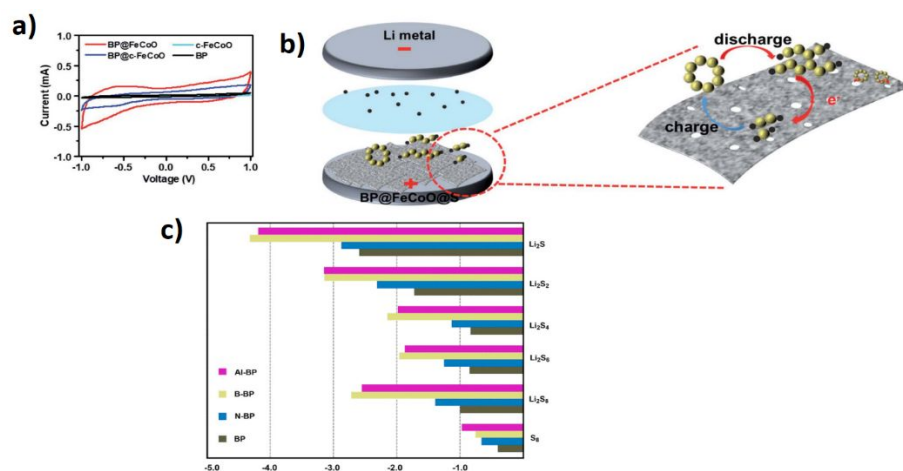


**Fig. 5.** a) CV curves of the symmetric cells using different materials as electrodes at a scan rate of  $10 \text{ mV s}^{-1}$ , Reproduced with permission from ref. **99**. Copyright 2018, Royal Society of Chemistry; b) Schematic illustration of the influence of the BP@FeCoO/S cathode on the shuttle of LiPSs and the conversion reaction kinetics of LiPSs, Reproduced with permission from ref. **99**. Copyright

2022, Royal Society of Chemistry c) Comparison of adsorption energy of polysulfides on BPs surfaces Reproduced with permission from ref. **106**. Copyright 2020, Elsevier.

The morphology, stability, polarity, catalytic ability and capacity retention for various 2D materials are shown in **Table 1**.

**Table 1: Morphologies, properties, and functions of 2D materials-based heterostructures**

Materials	Morphology	Stability	Polarity	Catalytic ability	Capacity retention	References
3D hierarchical nitrogen-doped graphene/CNTs	Microspheres	Good chemical stability	No	Low	77% after 500 cycles	<b>107</b>
Perovskite transition metal oxide (LaFeO <sub>3</sub> )	Nanofibers	Strong structural stability	Yes	Outstanding	62% after 500 cycles	<b>108</b>
Ni-doped MoS <sub>2</sub> (TMDs)	Nanosheets	Excellent cycling stability	Yes	Strong	85% after 100 cycles	<b>109</b>
Ti <sub>3</sub> C <sub>2</sub> T <sub>x</sub> (Freestanding MXene)	Nanofilm	Outstanding structural and cycling stability	Yes	Good	~85.2% after 500 cycles	<b>110</b>

MOFs/black phosphorus	Heterostructure	Superior thermal, air, dimensional and cycling stability	No	Outstanding	86.1 % after 100 cycles	111
-----------------------	-----------------	--	----	-------------	-------------------------	-----

2.6. hexagonal boron nitride (HBN)

Application of h-BN isoelectronic to graphene can overcome the limitations of graphene which are caused due to delicacy of single/few layers and tend to overlap and restack when fabricated into electrodes.<sup>112</sup>

Strong electrostatic attraction and noncovalent interaction of h-BN followed by innovative adsorptive property categorizes it as effective host for sulfur in lithium sulfur batteries. Associated challenge with wide bandgap of h-BN limits its application in Li-S batteries. However, the integration with other 2D nanomaterials could potentially overcome this challenge.<sup>113</sup>

The integration of graphene and h-BN has been recently investigated as host in lithium sulfur batteries to avoid polysulfide leakages. This composite (graphene/h-BN) combines the inherent adsorptive property of h-BN and higher conductivity of graphene. In a research study conducted by Fan et al., the charge transfer resistance of Li-S battery decreased using the functionalized boron nitride nanosheets/graphene. Moreover, the developed composite improved the cycling stability of investigated Li-S battery.<sup>114</sup>

Enhancement in the adsorption of polysulfides was proven by Deng et al. through the development of graphene-supported BN nanosheet composites in Li-S.<sup>115</sup> Mussa et al., developed RGO/h-BN

composite as sulfur hosts in Li-S batteries with enhanced electrochemical properties. Moreover, researchers proved a stable cycling performance at elevated temperatures.<sup>116</sup>

### 3. DFT and mechanism analysis for 2D materials (Heterostructures)

As shown in the previous sections, the possibilities for enhancing the performance of Li-S batteries are not limited by a few combinations, and it can be argued that the possibilities that may be explored are unlimited, which means the experimental investigation of all the possibilities cannot be achieved in a humanly possible time-frame. Therefore, computational materials science, ab-initio tools, and especially quantum mechanical methods such as density functional theory (DFT) can provide a high throughput highway for an accelerated atomic-scale materials design and discovery.<sup>117</sup>

DFT is now widely used for general battery design and well established in the mechanism analysis of 2D materials and Li-S batteries.<sup>118-121</sup> Through the calculation of chemical potentials, DFT can provide a concise overview of the open circuit potentials, and the feasibility of a cathode-anode couple.<sup>122</sup> DFT has also proven extremely effective in calculating diffusional pathways, and intercalation in any structure imaginable.<sup>123-125</sup> Calculation of the binding energies between any two species, such as  $\text{Li}_2\text{S}_n$  and the separator of any kind is also achieved through DFT.<sup>126</sup> It is now possible to calculate the impact of defects (point defects, or line defects) on the binding energies and the chemical potentials in a system as well, which opens the gateway for defect engineering in battery design.<sup>127-129</sup> In fact, it is possible to alter the stable defects in cathode or anode materials through heat treatments or irradiation, which warrants further computational insights.<sup>130</sup> DFT has been successfully used to predict finite-temperature defect equilibria as well.<sup>131, 132</sup> Various



dopants have been explored as mentioned in section 2, each of which contributes to the Li-S batteries in a unique way. Experimental analysis of defects can be extremely challenging; however, the fundamental impacts of the dopants and their defects on the electrochemical behavior of a system is calculable through DFT, by considering the electronic density of states, catalytic surface properties, defect formation energies, and the influence of the dopants on the binding energies.<sup>133-135</sup> Cathode and anode material generally suffer from volume changes during charging and discharging, which causes unwanted strains that ultimately result in premature failure. Calculating volumetric changes during charging/discharging, strain dependent phonon and the elastic properties are also possible through DFT, which can further aid in materials selection and battery design.<sup>136-138</sup> All of these possibilities can facilitate wide-scale investigations on a plethora of 2D heterostructures to find the optimum solutions prior to any experimental work, which can enormously accelerate our search for novel cathode-separator-anode combinations in Li-S batteries and beyond.

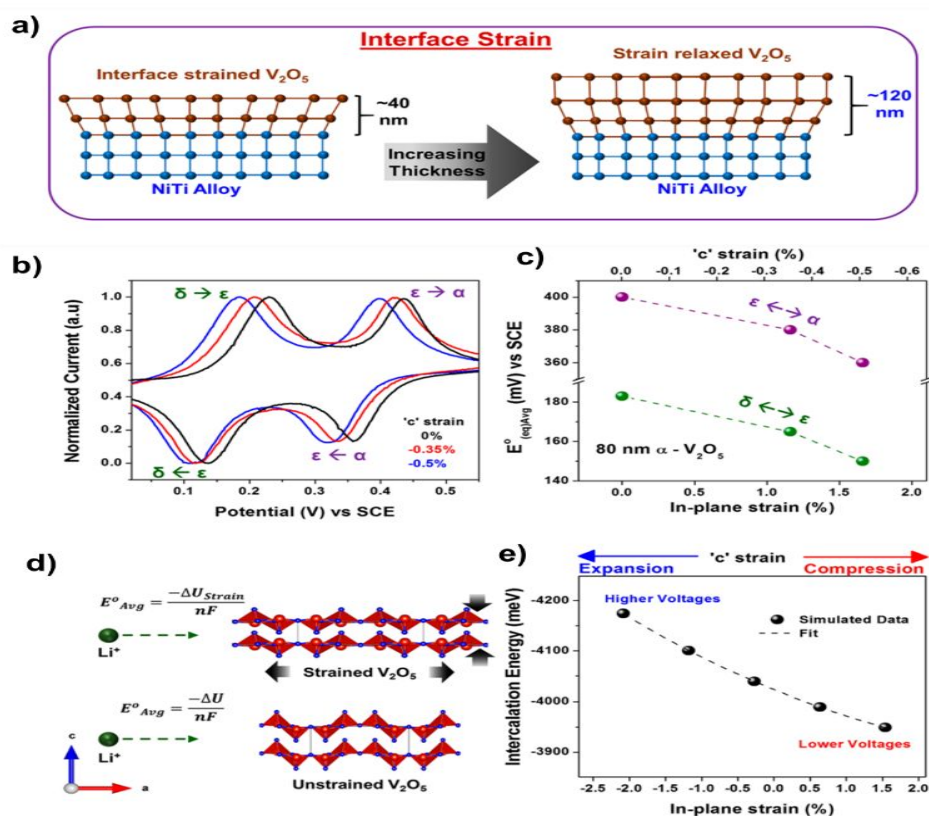


**Fig. 6.** a) Heterostructures will inevitably have strain effects at the interface, which impact the material properties, such as; b) normalized capacity; c)  $E^0$  vs SCE; d) interplanar spacing that affect diffusional pathways, and; e) intercalation energy. Reproduced with permission from ref. 144. Copyright 2017 ACS.

Two-dimensional Heterostructures are amongst the most attractive candidates for the future of battery design, which are also being actively explored through DFT, as shown by Bahari et al.<sup>139</sup> A heterostructures' properties may be estimated by the rule of mixtures, which has shown reasonable conformity with ab-initio simulations and experimental data for some combinations.<sup>140</sup> However, significant deviation in the materials properties of the hetero-structure couple from that of its constituents are known in the literature, the rule of mixtures cannot explain that. It is possible to explain such phenomena by the interfaces between the two structures (the heterojunctions) that are

a source for significant changes in the electronic behavior of the couple, and also the interfacial strain can completely transform the couple's interatomic spacing if the layers are in the order to several nm or less in thickness.<sup>141</sup> In case of 2D heterostructures, these effects can be even more drastic, and therefore, completely transforms the elastic properties, binding energies, electronic conductivities, diffusional pathways and all other materials properties, as the emerging field of strain engineering has shown in a wide range of materials.<sup>142,143</sup> DFT has proven to be an extremely powerful tool in the calculation of strain dependent materials properties for battery design as well, by using strain as a tuning factor for diffusion coefficients, open circuit potentials and other critical parameters, as shown in the **Fig. 6**.<sup>144</sup> In other words, a 2D heterostructures is a unique material from a theoretical perspective, and shouldn't be compared to its constituent members due to such interfacial strains, which can be an aid for tuning material properties by adjusting the strain in the heterostructures. Based on prior DFT calculations, the primary reasons for the behavior of this strain dependent material can be explained by the changes in the Fermi surfaces, electron localization function, and charge densities that the heterojunction causes.

A trailblazing methodology that has made DFT exponentially more effective is the introduction of artificial intelligence (AI) and machine learning (ML). One major disadvantage of DFT is the computational time required for atomistic quantum mechanical calculations. However, by using a limited dataset of DFT calculations as training data for a desired property, the computational time for prediction of properties such as binding energies can be reduced by 6 to 7 orders of magnitude, as shown by Zhang et al. on Li-S batteries (**Fig. 7**).<sup>145</sup> Therefore, by applying DFT-assisted ML, the search for extraordinary heterostructures is bound to gain an unprecedented pace.

Similarly, the sulphur and lithium adsorption sites can show a plethora of different configurations, as adsorption energies depend on the local chemical potential equilibria. This means, by bringing

1  
2  
3 together different combinations of phases in conjuncture with the 2D heterostructure, the S and Li  
4  
5 adsorption sites can be manipulated as well, to the advantage, as it was shown in our earlier study.  
6  
7 <sup>146</sup> One example that is of particular interest by Grixti et al.<sup>147</sup>, that shows the use of 2D boron for  
8  
9 the adsorption of polysulfides, that can reduce the shuttling effect. Their use of charge density  
10  
11 difference and calculation of binding energies, can be adopted to a plethora of other 2D materials  
12  
13 as well, that can accelerate the progress in Li-S batteries without shuttling effects. The evidence  
14  
15 regarding anchoring of polysulphides on 2D heterostructures are overwhelming, and also seen in  
16  
17 silicene and phosphorene, as reported by Li and Zhao <sup>148</sup>, which further necessitates a high-  
18  
19 throughput search using DFT.  
20  
21  
22  
23  
24  
25  
26  
27  
28  
29  
30  
31  
32  
33  
34  
35  
36  
37  
38  
39  
40  
41  
42  
43  
44  
45  
46  
47  
48  
49  
50  
51  
52  
53  
54  
55  
56  
57  
58  
59  
60

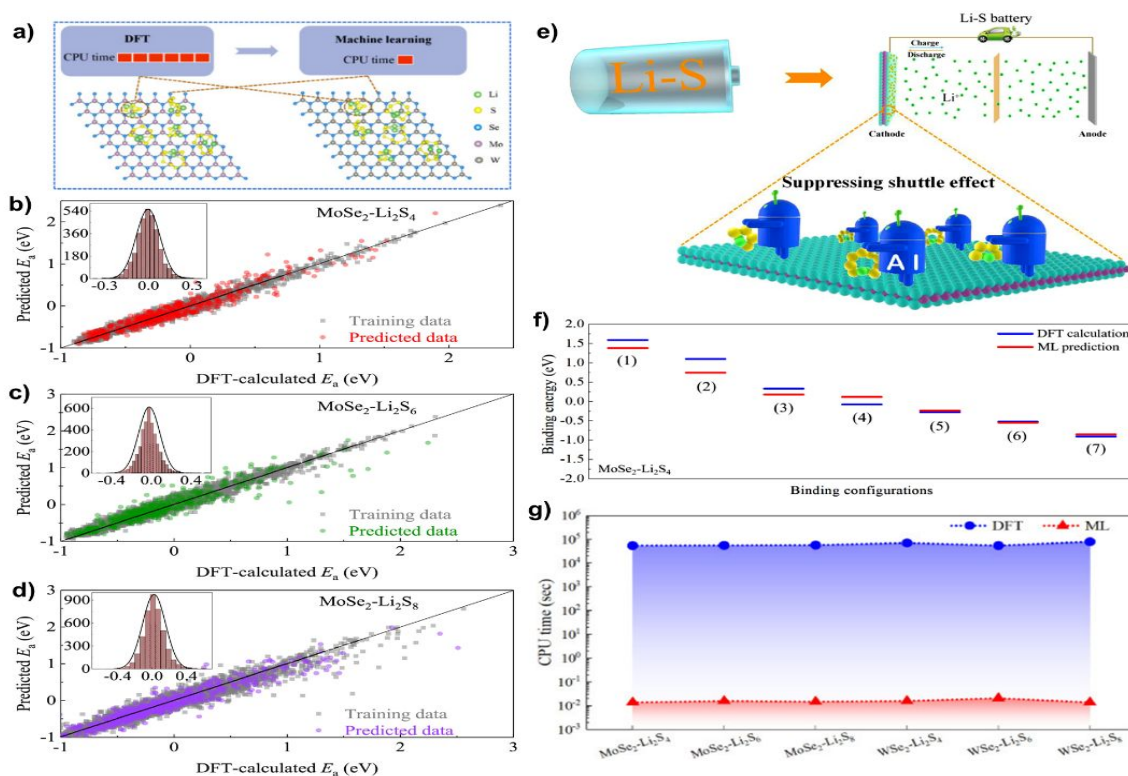


**Fig.7.** a) ML can effectively predict DFT calculated adsorption models, and adsorption energies that are reasonably close to their DFT calculated counterparts in; b)  $\text{MoSe}_2\text{-Li}_2\text{S}_4$ ; c)  $\text{MoSe}_2\text{-Li}_2\text{S}_6$ ; d)  $\text{MoSe}_2\text{-Li}_2\text{S}_8$ . e) AI can be trained based on DFT data to predict shuttle effects in Li-S batteries; f) while providing binding energies that are acceptable; g) The computational time required for ML calculations is 6 to 7 orders of magnitude faster than DFT. Reproduced with permission from ref. 145. Copyright 2021, Elsevier.

#### 4. Properties of 2-D Heterostructures (flexibility, dendrite growth, self-assembly)

1  
2  
3 It was discovered that graphene serves as a suitable material for immobilizing LiPSs. In sulfur  
4 cathodes, LiPSs are frequently utilized and graphene can effectively accommodate them due to its  
5 ample space. The Li-S battery was designed by Cheng's team using a new approach. Sulfur and  
6 graphene are utilized in the design of a PP separator, rather than relying on aluminum foil. Vacuum  
7 filtration was utilized in its creation.<sup>149</sup>  
8  
9

10  
11  
12  
13  
14  
15 The addition of a graphene layer acted as a barrier to unwanted lithium sulfur intermediates,  
16 keeping the sulfur battery protected. Its function was also to serve as a barrier that hindered the  
17 quick diffusion of polysulfides. The battery was able to retain a significant amount of capacity  
18 over a prolonged cycle life. Despite being used 500 cycles, it only lost a negligible amount of  
19 capacity fade with every cycle. The introduction of lithium-sulfur batteries with 2D graphene are  
20 investigated to generate batteries with enhanced strength and flexibility that could store more  
21 energy.<sup>150</sup>  
22  
23  
24  
25  
26  
27  
28  
29  
30

31  
32 2D materials may enhance the performance of sulfur batteries through the creation of flexible  
33 pathways that facilitate faster electron flow. To achieve this rephrasing, the materials are either  
34 stacked or linked together. Self-assembly can create unique surface properties and miniaturized  
35 holes in the materials by arranging them in a particular manner. The reaction that occurs when  
36 using LiPS batteries can be accelerated by certain materials. Their flatness and durability make  
37 these materials exceptionally robust. The recent discovery of ultrathin sheets known as MXenes  
38 has aroused great interest. There is a lot of interest in materials that have a two-dimensional shape  
39 similar to graphene. Mxenes have high conductivity, electricity, naturally flexible and physically  
40 strong. MXenes have the potential to produce flexible electrodes with their large interlayer  
41 channels.<sup>151</sup>  
42  
43  
44  
45  
46  
47  
48  
49  
50  
51  
52  
53  
54  
55  
56  
57  
58  
59  
60

It was found that the Graphene, as a 2D material with high specific surface area and electrical conductivity could restrain the dendrite growth and increase electrode surface area.

Mukherjee et al. synthesized a porous graphene networks (PGN). The porous graphene induced the homogeneous deposition and served as a caged entrapment for lithium resulting in increased Coulombic efficiency and suppressed dendrite growth.<sup>152</sup>

Sulfur and 2D materials offer a means to produce self- assemble pathways that facilitate rapid movement of electrons and ions. Materials are combined through stacking or linking to achieve this. Irrespective of the method of growth, 2D material heterostructures will provide self–assembly feature in order to conserve energy.<sup>153</sup> Spontaneous alignment can aid in the creation of small objects. Their excellent electrical properties lead to potential for new discoveries. The growth of 2D materials can aid in the visualization of their grain structures. The behavior of materials is highly impacted by these structures.

**5. Challenges and Perspectives**

Using 2D material based heterostructures in cathodes and separators of Li-S batteries is a promising approach due to their high surface area, strength, outstanding thermal conductivity, and self-assembly properties. The high surface area enhances active material utilization in the cathode, while the high strength and thermal conductivity improve the mechanical stability and thermal management. In separators, the self-assembly properties of 2D materials lead to a highly porous and ordered structure, enhancing ionic conductivity. The unique properties of 2D materials make them ideal for battery applications, and further research is expected to improve performance. Different types of 2D materials, such as graphene and its derivatives, TMOs, TMDs, MXenes, and

BP, have been summarized in this review. The well-organized graphene structures successfully encapsulated the dissolute polysulfides and promoted the movement of electrons and mass. Doped heteroatoms on graphene typically form chemical interactions with sulfur and lithium polysulfides. The utilization of nitrogen-doped graphene as the Li-S cathode host was investigated and several heteroatoms have been used, such as nitrogen, sulfur, phosphorus, indium, Fe and boron.

Modifying the hierarchical structure of 2D material based heterostructures, such as graphene or MXenes are a useful strategy for improving the performance of Li-S batteries. Modifying the hierarchical structure of 2D material based heterostructures, such as graphene or MXenes is a useful strategy for improving the performance of Li-S batteries. By controlling the size and distribution of the conductive material and the binder in the cathode, it is possible to reduce the formation of voids and improve the mechanical stability of the battery. Using 2D materials with high conductivity can also increase the overall efficiency of the battery. This approach is promising for further research and development.

2D materials (TMOs and TMDs) with numerous active sites and functional groups display anchoring sites for polysulfide. Functional groups can modify the active sites on 2D materials to control the nucleation and growth of polysulfides. This review provides an overview of recent advancements in utilizing heterostructures of two-dimensional (2D) materials for Li-S batteries, with the aim of enhancing battery performance and stability. These advancements encompass various strategies, including modifying the hierarchical structure of the cathode to efficiently accommodate sulfur, as well as employing 2D materials with high conductivity. Additionally, incorporating 2D material heterostructures into separators improves ionic conductivity. Moreover, exploiting the extensive surface area and self-assembly properties of 2D materials has been shown to enhance battery performance. These promising advancements indicate the potential for further



improvements in the performance and stability of Li-S batteries through ongoing research. We presented and classified some carefully chosen 2D materials with distinct characteristics. To address the issues of insulating intermediates, polysulfides shuttle and slow kinetics, we summarized strategies for utilizing the interesting characteristics of 2D material based heterostructures such as superior conductivity, selectable functional groups and good flexibility for enhancing electrochemical performance.

Utilizing 2D material-based heterostructures in both cathodes and separators of Li-S batteries holds promise due to the exceptional surface area, strength, outstanding thermal conductivity, and self-assembly properties exhibited by these materials. The increased surface area improves the utilization of active materials within the cathode, while the enhanced mechanical stability and thermal management resulting from the high strength and thermal conductivity contribute to overall battery performance. In separators, the self-assembly properties of 2D materials facilitate the formation of highly porous and ordered structures, thereby augmenting ionic conductivity. Consequently, the unique properties of 2D materials render them highly suitable for battery applications, and further research is anticipated to enhance their performance. This review summarizes various types of 2D materials, such as graphene and its derivatives, transition metal oxides (TMOs), transition metal dichalcogenides (TMDs), MXenes, and black phosphorus (BP), along with their relevant characteristics. Graphene-based structures, for instance, have been successfully employed to encapsulate dissolute polysulfides and facilitate the movement of electrons and mass. Nitrogen-doped graphene has been investigated as a cathode host for Li-S batteries, with various heteroatoms, including nitrogen, sulfur, phosphorus, indium, iron, and boron, being utilized.

The addition of TMOs introduces strong polar interactions between electron-attractive metals and negatively charged polysulfides, as well as between oxygens and  $\text{Li}^+$  ions. TMOs based on manganese (Mn) and titanium (Ti) have recently garnered considerable attention due to their remarkable ability to restrain polysulfides. TMDs, exhibiting a graphene-like structure with distinctive physical properties, excellent structural stability, and abundant transition metal d-electrons, constitute a notable family of polar materials. Among the stacked TMDs, titanium disulfide ( $\text{TiS}_2$ ) stands out for its lowest weight, cost, highest stability, and superior binding affinity to polysulfides. Functionalizing MXenes with various functional groups such as hydroxyl (OH), oxygen (O), chlorine (Cl), and fluorine (F) enhances their hydrophilicity. In particular, MXene surface groups, notably hydroxyl groups, exhibit a strong affinity for polysulfides and can attract them without requiring additional surface modifications. Additionally, the highly conductive core of MXenes, comprising titanium-carbon (Ti C Ti) bonds, accelerates charge transfer kinetics, thereby significantly improving sulfur utilization and capacity retention.

BP, with its high electrical conductivity and rapid Li-ion transport, possesses numerous active sites along its edges, affording remarkable chemisorptive potential for LiPSs. The surface technique of aluminum doping of BP has shown promise in enhancing BP performance and reducing loading.

Another strategy for enhancing Li-S battery performance is the modification of the hierarchical structure of 2D material-based heterostructures, such as graphene or MXenes. By carefully controlling the size and distribution of conductive materials and binders in the cathode, void formation can be minimized, thereby improving battery mechanical stability. Furthermore,

employing 2D materials with high conductivity can enhance overall battery efficiency. These approaches hold significant promise for future research and development efforts.

## 6. Summary and Conclusion

In this review, we summarized recent advances in the use of 2D material heterostructures for Li-S batteries. Recent advances in the use of 2D material heterostructures for Li-S batteries aim to improve performance and stability. Strategies include modifying the cathode's hierarchical structure to host sulfur efficiently and using 2D materials with high conductivity. In separators, 2D material heterostructures enhance ionic conductivity. Utilizing 2D materials' high surface area and self-assembly properties is also shown to enhance battery performance. These advances show promise, and further research is expected to lead to even more Li-S battery performance and stability improvements. We presented and classified some carefully chosen 2D materials with distinct characteristics. To address the issues of insulating intermediates, polysulfides shuttle and slow kinetics, we summarized strategies for utilizing the interesting characteristics of 2D material based heterostructures such as superior conductivity, selectable functional groups and good flexibility for enhancing electrochemical performance.

Detecting redox reactions in Li-S batteries is important for understanding their performance and stability, but conventional characterization techniques are limited in their ability to detect these reactions accurately. Novel techniques such as operando spectroscopy and high-resolution microscopy provide real-time information about the redox reactions and are crucial for detecting and understanding the reactions in Li-S batteries. These techniques can improve the optimization of battery design and overall performance. In situ atomic force microscopy (AFM), X-ray diffraction (XRD) and in situ transmission electron microscopy (TEM) should investigate. To

1  
2  
3 directly accelerate the sluggish steps and to achieve high-rate capabilities, one optimal strategy is  
4 to explore new and efficient catalysts and to apply them in lithium– sulfur batteries.  
5

6  
7 The thermal conductivity of 2D materials should be mentioned to mitigate lithium dendrites.  
8  
9 Modifying the thermal conductivity of 2D material-based heterostructures is a promising strategy  
10 for improving the lifespan of Li-S batteries. This is because thermal management is crucial for  
11 maintaining the performance and stability of Li-S batteries, as the accumulation of heat can lead  
12 to thermal runaway and shorten the battery's lifespan. By integrating high thermal conductivity 2D  
13 materials into the battery structure, it is possible to enhance the dissipation of heat and improve  
14 the thermal stability of the battery. The combination of different 2D materials in heterostructures  
15 can also result in a composite material with even higher thermal conductivity, further enhancing  
16 the thermal stability of Li-S batteries.  
17  
18  
19  
20  
21  
22  
23  
24  
25  
26  
27  
28  
29

30 Detecting and comprehending redox reactions in Li-S batteries is crucial for understanding their  
31 performance and stability. However, conventional characterization techniques have limitations in  
32 accurately detecting these reactions. Novel techniques, including operando spectroscopy and  
33 high-resolution microscopy, provide real-time insights into redox reactions, enabling accurate  
34 detection and understanding of these processes in Li-S batteries. These techniques facilitate the  
35 optimization of battery design and overall performance. Additionally, in situ atomic force  
36 microscopy (AFM), X-ray diffraction (XRD), and in situ transmission electron microscopy  
37 (TEM) are recommended for further investigation. Exploring new and efficient catalysts, as well  
38 as their application in lithium-sulfur batteries, represents an optimal strategy for directly  
39 accelerating sluggish steps and achieving high-rate capabilities.  
40  
41  
42  
43  
44  
45  
46  
47  
48  
49  
50  
51  
52  
53  
54  
55  
56  
57  
58  
59  
60

1  
2  
3  
4  
5  
6  
7  
8  
9  
10  
11  
12  
13  
14  
15  
16  
17  
18  
19  
20  
21  
22  
23  
24  
25  
26  
27  
28  
29  
30  
31  
32  
33  
34  
35  
36  
37  
38  
39  
40  
41  
42  
43  
44  
45  
46  
47  
48  
49  
50  
51  
52  
53  
54  
55  
56  
57  
58  
59  
60

Considering the mitigation of lithium dendrites, thermal conductivity of 2D materials should be addressed. Modifying the thermal conductivity of 2D material-based heterostructures emerges as a promising strategy for prolonging the lifespan of Li-S batteries. Efficient thermal management is crucial to maintain battery performance and stability, as excessive heat accumulation can lead to thermal runaway and shorten battery lifespan. By incorporating 2D materials with high thermal conductivity into the battery structure, heat dissipation can be enhanced, thereby improving thermal stability. Combining different 2D materials in heterostructures can yield composite materials with even higher thermal conductivity, further augmenting the thermal stability of Li-S batteries.

**Conflict of Interest**

The authors declare no competing interest.

**Acknowledgements**

All authors would like to thank University College of Dublin-Ireland, Indian Institute of Technology Jodhpur-India, Czech Technical University in Prague , University of Southampton-United Kingdom for resource and technical support.

**Dr. Maryam Sadat Kiai** is a postdoctoral researcher in University College Dublin, undertaking research activities at the Centre for BioNano Interactions. She received her Ph.D. in Nano Science and Nano Engineering from Istanbul Technical University. The nature of her PhD degree involved a great deal of research on nanofabrication techniques for the next generation of rechargeable batteries. Dr. Maryam has published more than 30 high-quality papers as well as one book chapter.

**Dr. Srikanth Ponnada MRSC** is currently Post-doctoral Fellow at Chemical and Biological Engineering Department, Colorado School of Mines-U.S.A. Previously he worked as Postdoctoral Research Associate at Indian Institute of Technology Jodhpur-Rajasthan. His current research area includes Functional materials synthesis, Polymer electrolyte membranes and device fabrication, Energy storage, Conversion devices (fuel cells), Electrochemical sensors and Electrocatalysis.

**Mubashir Mansoor** is a PhD candidate in the materialsscience and engineering program of the Istanbul Technical University (ITU), in Turkey. His research isfocused on the study of point defects and finite temperaturedefect transformations through *ab-initio* methods such asdensity functional theory coupled with various experimental approaches including heat treatments.

**Dr. Navid Aslfattahi**, has received his Ph.D. in Mechanical Engineering from University of Malaya-Malaysia. Currently, he is Postdoctoral Scholar in the Institute of Fluid Mechanics and thermodynamics, Czech Technical University in Prague. Dr. Navid has published more than 65 ISI/Scopus indexed high quality papers and h-index of 25 as well as two book chapters. His research interest area includes energy storage materials, energy efficiency, solar thermal systems, nanocomposites, MXene, 2D nanoparticles, batteries and fuel cells.

**Dr. Susmita Naskar**, FHEA is an assistant professor in Faculty of Engineering and Physical Sciences at University of Southampton, UK. Dr Naskar is the founding director of Engineered Materials and Structures Laboratory at University of Southampton. Her primary area of interest is the multi scale and multi-physics analysis of physical systms, with mechanics as its epicentre. Dr. Naskar's research findings and developments are regularly published in reputed journals and conferences.

## References

1. Xu, H., Kong, Z., Siegenthaler, J., Zheng, B., Tong, Y., Li, J., Schuelke, T., Fan, Q.H., Wang, K., Xu, H. and Jin, H. Review on recent advances in two-dimensional nanomaterials-based cathodes for lithium-sulfur batteries. *EcoMat.* **2023**, e12286.
2. Zhao, F., Xue, J., Shao, W., Yu, H., Huang, W. and Xiao, J. Toward high-sulfur-content, high-performance lithium-sulfur batteries: Review of materials and technologies. *Journal of Energy Chemistry.* **2023**.
3. Kiai, M.S., Mansoor, M., Ponnada, S., Gorle, D.B., Aslfattahi, N. and Sharma, R.K. Integration of PDAAQ and Non-stoichiometric MgO as Host Cathode Materials for Lithium-Sulfur Batteries with Superior Cycle Stability: Density Functional Theory Calculations and Experimental Validations. *Energy & Fuels.* **2022**, 36(24), 15199-15209.
4. Ali, T. and Yan, C. 2 D materials for inhibiting the shuttle effect in advanced lithium-sulfur batteries. *ChemSusChem.* **2020**, 13(6), 1447-1479.
5. Zhou, T., Lv, W., Li, J., Zhou, G., Zhao, Y., Fan, S., Liu, B., Li, B., Kang, F. and Yang, Q.H. Twinborn TiO<sub>2</sub>-TiN heterostructures enabling smooth trapping-diffusion-conversion of polysulfides towards ultralong life lithium-sulfur batteries. *Energy & Environmental Science.* **2017**, 10(7), 1694-1703.
6. Song, Y., Zhao, W., Kong, L., Zhang, L., Zhu, X., Shao, Y., Ding, F., Zhang, Q., Sun, J. and Liu, Z. Synchronous immobilization and conversion of polysulfides on a VO<sub>2</sub>-VN binary host targeting high sulfur load Li-S batteries. *Energy & Environmental Science.* **2018**, 11(9), 2620-2630.
7. Ji, L., Rao, M., Zheng, H., Zhang, L., Li, Y., Duan, W., Guo, J., Cairns, E.J. and Zhang, Y. Graphene oxide as a sulfur immobilizer in high performance lithium/sulfur cells. *Journal of the American Chemical Society.* **2011**, 133(46), 18522-18525.
8. Qiu, Y., Li, W., Zhao, W., Li, G., Hou, Y., Liu, M., Zhou, L., Ye, F., Li, H., Wei, Z. and Yang, S., High-rate, ultralong cycle-life lithium/sulfur batteries enabled by nitrogen-doped graphene. *Nano letters.* **2014**, 14(8), pp.4821-4827.
9. Bao, W., Liu, L., Wang, C., Choi, S., Wang, D. and Wang, G. Facile synthesis of crumpled nitrogen-doped mxene nanosheets as a new sulfur host for lithium-sulfur batteries. *Advanced Energy Materials.* **2018**, 8(13), 1702485.

10. Manthiram, A., Fu, Y., Chung, S.H., Zu, C. and Su, Y.S. Rechargeable lithium–sulfur batteries. *Chemical reviews*. **2014**, *114*(23), 11751-11787.
11. Li, B., Xu, H., Ma, Y. and Yang, S. Harnessing the unique properties of 2D materials for advanced lithium–sulfur batteries. *Nanoscale horizons*. **2019**, *4*(1), 77-98.
12. Rauh, R.D., Abraham, K.M., Pearson, G.F., Surprenant, J.K. and Brummer, S.B. A lithium/dissolved sulfur battery with an organic electrolyte. *Journal of the Electrochemical Society*. **1979**, *126*(4), 523.
13. Childress, A.S., Parajuli, P., Zhu, J., Podila, R. and Rao, A.M. A Raman spectroscopic study of graphene cathodes in high-performance aluminum ion batteries. *Nano Energy*. **2017**, *39*, 69-76.
14. Raccichini, R., Varzi, A., Wei, D. and Passerini, S. Critical insight into the relentless progression toward graphene and graphene-containing materials for lithium-ion battery anodes. *Advanced materials*. **2017**, *29*(11), 1603421.
15. Lotya, M., Hernandez, Y., King, P.J., Smith, R.J., Nicolosi, V., Karlsson, L.S., Blighe, F.M., De, S., Wang, Z., McGovern, I.T. and Duesberg, G.S. Liquid phase production of graphene by exfoliation of graphite in surfactant/water solutions. *Journal of the American Chemical Society*. **2009**, *131*(10), 3611-3620.
16. Xue, Y., Zhang, Q., Wang, W., Cao, H., Yang, Q. and Fu, L. Opening two-dimensional materials for energy conversion and storage: A concept. *Advanced Energy Materials*. **2017**, *7*(19), 1602684.
17. Raccichini, R., Varzi, A., Passerini, S. and Scrosati, B., *Nature Mater*. **2015**, *14*, 271.
18. Cong, L., Xie, H. and Li, J. Hierarchical structures based on two-dimensional nanomaterials for rechargeable lithium batteries. *Advanced Energy Materials*. **2017**, *7*(12), 1601906.
19. Hou, H., Qiu, X., Wei, W., Zhang, Y. and Ji, X. Carbon anode materials for advanced sodium-ion batteries. *Advanced energy materials*. **2017**, *7*(24), 1602898.
20. Mei, J., Liao, T., Kou, L. and Sun, Z. Two-dimensional metal oxide nanomaterials for next-generation rechargeable batteries. *Advanced Materials*. **2017**, *29*(48), 1700176.
21. Liu, Y., Wu, J., Hackenberg, K.P., Zhang, J., Wang, Y.M., Yang, Y., Keyshar, K., Gu, J., Ogitsu, T., Vajtai, R. and Lou, J. Self-optimizing, highly surface-active layered metal dichalcogenide catalysts for hydrogen evolution. *Nature Energ*. **2017**, *2*(9), 1-7.



22. Yun, Q., Lu, Q., Zhang, X., Tan, C. and Zhang, H. Three-dimensional architectures constructed from transition-metal dichalcogenide nanomaterials for electrochemical energy storage and conversion. *Angewandte Chemie International Edition*. **2018**, 57(3), 626-646.
23. Gao, Y.P., Wu, X., Huang, K.J., Xing, L.L., Zhang, Y.Y. and Liu, L. Two-dimensional transition metal diseleniums for energy storage application: a review of recent developments. *CrystEngComm*. **2017**, 19(3), 404-418.
24. Anasori, B., Lukatskaya, M.R. and Gogotsi, Y. 2D metal carbides and nitrides (MXenes) for energy storage. *Nature Reviews Materials*. **2017**, 2(2), 1-17.
25. Sun, J., Lee, H.W. and Pasta, M. HY uan, G. Zheng, Y. Sun, Y. Li and Y. Cui. *Nat. Nanotechnol.* **2015**, 10(11), 980-985.
26. Ding, L., Wei, Y., Wang, Y., Chen, H., Caro, J. and Wang, H. A two-dimensional lamellar membrane: MXene nanosheet stacks. *Angewandte Chemie International Edition*. **2017**, 56(7), 1825-1829.
27. Fang, R., Zhao, S., Pei, S., Qian, X., Hou, P.X., Cheng, H.M., Liu, C. and Li, F. Toward more reliable lithium–sulfur batteries: an all-graphene cathode structure. *ACS nano*. **2016**, 10(9), 8676-8682.
28. Zhao, M.Q., Sedran, M., Ling, Z., Lukatskaya, M.R., Mashtalir, O., Ghidui, M., Dyatkin, B., Tallman, D.J., Djenizian, T., Barsoum, M.W. and Gogotsi, Y. Inside Cover: Synthesis of Carbon/Sulfur Nanolaminates by Electrochemical Extraction of Titanium from Ti<sub>2</sub>SC (Angew. Chem. Int. Ed. 16/2015). *Angewandte Chemie International Edition*. **2015**, 54(16), 4682-4682.
29. Zhou, G., Paek, E., Hwang, G.S. and Manthiram, A. Long-life Li/polysulphide batteries with high sulphur loading enabled by lightweight three-dimensional nitrogen/sulphur-codoped graphene sponge. *Nature communications*. **2015**, 6(1), 7760.
30. Li, G., Sun, J., Hou, W., Jiang, S., Huang, Y. and Geng, J. Three-dimensional porous carbon composites containing high sulfur nanoparticle content for high-performance lithium–sulfur batteries. *Nature communications*. **2016**, 7(1), 10601.
31. Zhao, Y., Feng, J., Liu, X., Wang, F., Wang, L., Shi, C., Huang, L., Feng, X., Chen, X., Xu, L. and Yan, M. Self-adaptive strain-relaxation optimization for high-energy lithium storage material through crumpling of graphene. *Nature communications*. **2014**, 5(1), 4565.

32. Lin, T., Tang, Y., Wang, Y., Bi, H., Liu, Z., Huang, F., Xie, X. and Jiang, M. Scotch-tape-like exfoliation of graphite assisted with elemental sulfur and graphene–sulfur composites for high-performance lithium-sulfur batteries. *Energy & Environmental Science*. **2013**, 6(4), 1283-1290.
33. Hao, G.P., Tang, C., Zhang, E., Zhai, P., Yin, J., Zhu, W., Zhang, Q. and Kaskel, S. Thermal exfoliation of layered metal–organic frameworks into ultrahydrophilic graphene stacks and their applications in Li–S batteries. *Advanced Materials*. **2017**, 29(37), 1702829.
34. Chen, H., Chen, C., Liu, Y., Zhao, X., Ananth, N., Zheng, B., Peng, L., Huang, T., Gao, W. and Gao, C. High-quality graphene microflower design for high-performance Li–S and Al-ion batteries. *Advanced Energy Materials*. **2017**, 7(17), 1700051.
35. Xu, G., Yuan, J., Geng, X., Dou, H., Chen, L., Yan, X. and Zhu, H. Caterpillar-like graphene confining sulfur by restacking effect for high performance lithium sulfur batteries. *Chemical Engineering Journal*. **2017**, 322, 454-462.
36. Zhang, X., Zhang, Z. and Zhou, Z. MXene-based materials for electrochemical energy storage. *Journal of energy chemistry*. **2018**, 27(1), 73-85.
37. Zu, C. and Manthiram, A. Hydroxylated graphene–sulfur nanocomposites for high-rate lithium–sulfur batteries. *Advanced Energy Materials*. **2013**, 3(8), 1008-1012.
38. Xu, J., Shui, J., Wang, J., Wang, M., Liu, H.K., Dou, S.X., Jeon, I.Y., Seo, J.M., Baek, J.B. and Dai, L. Sulfur–graphene nanostructured cathodes via ball-milling for high-performance lithium–sulfur batteries. *ACS nano*. **2014**, 8(10), 10920-10930.
39. Park, M.S., Yu, J.S., Kim, K.J., Jeong, G., Kim, J.H., Jo, Y.N., Hwang, U.K., Kang, S., Woo, T. and Kim, Y.J. One-step synthesis of a sulfur-impregnated graphene cathode for lithium–sulfur batteries. *Physical Chemistry Chemical Physics*. **2012**, 14(19), 6796-6804.
40. Song, J., Xu, T., Gordin, M.L., Zhu, P., Lv, D., Jiang, Y.B., Chen, Y., Duan, Y. and Wang, D., Nitrogen-doped mesoporous carbon promoted chemical adsorption of sulfur and fabrication of high-areal-capacity sulfur cathode with exceptional cycling stability for lithium-sulfur batteries. *Advanced functional materials*. **2014**, 24(9), 1243-1250.
41. Song, J., Yu, Z., Gordin, M.L. and Wang, D.. Advanced sulfur cathode enabled by highly crumpled nitrogen-doped graphene sheets for high-energy-density lithium–sulfur batteries. *Nano letters*. **2016**, 16(2), 864-870.

42. Cheng, X., Chen, R., Zhu, X., Liao, Q., An, L., Ye, D., He, X., Li, S. and Li, L. An optofluidic planar microreactor for photocatalytic reduction of CO<sub>2</sub> in alkaline environment. *Energy*, **2017**, *120*, 276-282.
43. Ma, Z., Dou, S., Shen, A., Tao, L., Dai, L. and Wang, S. Sulfur-doped graphene derived from cycled lithium-sulfur batteries as a metal-free electrocatalyst for the oxygen reduction reaction. *Angewandte Chemie*. **2015**, *127*(6), 1908-1912.
44. Wu, H., Xia, L., Ren, J., Zheng, Q., Xu, C. and Lin, D. A high-efficiency N/P co-doped graphene/CNT@ porous carbon hybrid matrix as a cathode host for high performance lithium-sulfur batteries. *Journal of Materials Chemistry A*. **2017**, *5*(38), 20458-20472.
45. Xiao, Z., Yang, Z., Zhang, L., Pan, H. and Wang, R. Sandwich-type NbS<sub>2</sub>@ S@ I-doped graphene for high-sulfur-loaded, ultrahigh-rate, and long-life lithium-sulfur batteries. *ACS nano*. **2017**, *11*(8), 8488-8498.
46. Eroglu, O., Kiai, M.S. and Kizil, H. Performance enhancement of Li-S battery with the anatase nano structured Fe doped TiO<sub>2</sub> as a robust interlayer. *Journal of Alloys and Compounds*. **2020**, *838*, 155607.
47. Kaiser, M.R., Ma, Z., Wang, X., Han, F., Gao, T., Fan, X., Wang, J.Z., Liu, H.K., Dou, S. and Wang, C. Reverse microemulsion synthesis of sulfur/graphene composite for lithium/sulfur batteries. *ACS nano*. **2017**, *11*(9), 9048-9056.
48. Eroglu, O., Kiai, M.S. and Kizil, H. Glass fiber separator coated by boron doped anatase TiO<sub>2</sub> for high-rate Li-S battery. *Materials Research Bulletin*. **2020**, *129*, 110917.
49. Hou, T.Z., Xu, W.T., Chen, X., Peng, H.J., Huang, J.Q. and Zhang, Q. Lithium bond chemistry in lithium-sulfur batteries. *Angewandte Chemie*. **2017**, *129*(28), 8290-8294.
50. Kiai, M.S. and Kizil, H. Enhanced performance of Li-S battery with polymer doped potassium functionalized graphene interlayers as effective polysulfide barrier. *Journal of Electroanalytical Chemistry*. **2019**, *851*, 113405.
51. Ponnada, S., Kiai, M.S., Gorle, D.B. and Nowduri, A. Application of Facile Graphene Oxide Binders with Nanocomposites for Efficient Separator Performance in Lithium Sulfur Batteries. *Energy & Fuel*. **2021**, *35*(15), 12619-12627.
52. Jin, C., Sheng, O., Zhang, W., Luo, J., Yuan, H., Yang, T., Huang, H., Gan, Y., Xia, Y., Liang, C. and Zhang, J. Sustainable, inexpensive, naturally multi-functionalized biomass carbon for both Li metal anode and sulfur cathode. *Energy Storage Materials*. **2018**, *15*, 218-225.

53. Wang, R., Yang, J., Chen, X., Zhao, Y., Zhao, W., Qian, G., Li, S., Xiao, Y., Chen, H., Ye, Y. and Zhou, G. Highly dispersed cobalt clusters in nitrogen-doped porous carbon enable multiple effects for high-performance Li–S battery. *Advanced Energy Materials*. **2020**, 10(9), 1903550.
54. Kiai, M.S., Eroglu, O. and Kizil, H. Polycarboxylate functionalized graphene/S composite cathodes and modified cathode-facing side coated separators for advanced lithium-sulfur batteries. *Nanoscale Research Letters*. **2019**, 14(1), 1-11.
55. SPonnada, S., Kiai, M.S., Gorle, D.B. and Nowduri, A. Improved performance of lithium–sulfur batteries by employing a sulfonated carbon nanoparticle-modified glass fiber separator. *Nanoscale Advances*. **2021**, 3(15), 4492-4501.
56. Zhang, M., Wang, L., Wang, B., Zhang, B., Sun, X., Wang, D., Kong, Z. and Xu, L. Phosphorus-modified Fe 4 N@ N, P co-doped graphene as an efficient sulfur host for high-performance lithium–sulfur batteries. *Journal of Materials Chemistry A*, **2021**, 9(10), 6538-6546.
57. Liu, X., Huang, J.Q., Zhang, Q. and Mai, L. Nanostructured metal oxides and sulfides for lithium–sulfur batteries. *Advanced materials*. **2017**, 29(20), 1601759.
58. Liang, D., DeGrave, J.P., Stolt, M.J., Tokura, Y. and Jin, S. Current-driven dynamics of skyrmions stabilized in MnSi nanowires revealed by topological Hall effect. *Nature communications*. **2015**, 6(1), 8217.
59. Li, M., Dai, Y., Pei, X. and Chen, W. Hierarchically porous  $\gamma$ -Ti<sub>3</sub>O<sub>5</sub> hollow nanospheres as an effective sulfur host for long-life lithium-sulfur batteries. *Applied Surface Science*. **2022**, 579, 152178.
60. Liang, X. and Nazar, L.F. In situ reactive assembly of scalable core–shell sulfur–MnO<sub>2</sub> composite cathodes. *ACS nano*. **2016**, 10(4), 4192-4198.
61. Benítez, A., Amaro-Gahete, J., Chien, Y.C., Caballero, Á., Morales, J. and Brandell, D. Recent advances in lithium-sulfur batteries using biomass-derived carbons as sulfur host. *Renewable and Sustainable Energy Reviews*. **2022**, 154, 111783.
62. Marangon, V., Hernández-Rentero, C., Olivares-Marín, M., Gómez-Serrano, V., Caballero, Á., Morales, J. and Hassoun, J. A Stable High-Capacity Lithium-Ion Battery Using a Biomass-Derived Sulfur-Carbon Cathode and Lithiated Silicon Anode. *ChemSusChem*. **2021**, 14(16), 3333-3343.
63. Eng, A.Y.S., Kumar, V., Zhang, Y., Luo, J., Wang, W., Sun, Y., Li, W. and Seh, Z.W. Room-temperature sodium–sulfur batteries and beyond: realizing practical high energy systems

through anode, cathode, and electrolyte engineering. *Advanced Energy Materials*. **2021**, 11(14), 2003493.

64. Ye, Y., Wu, F., Xu, S., Qu, W., Li, L. and Chen, R. Designing realizable and scalable techniques for practical lithium sulfur batteries: a perspective. *The Journal of Physical Chemistry Letters*. **2018**, 9(6), 1398-1414.

65. Ge, Y., Chen, P., Zhang, W., Shan, Q., Fang, Y., Chen, N., Yuan, Z., Zhang, Y. and Feng, X. Shape-controlled MnO<sub>2</sub> as a sulfur host for high performance lithium–sulfur batteries. *New Journal of Chemistry*. **2020**, 44(26), 11365-11372.

66. Kang, Z., Wu, C., Dong, L., Liu, W., Mou, J., Zhang, J., Chang, Z., Jiang, B., Wang, G., Kang, F. and Xu, C. 3D porous copper skeleton supported zinc anode toward high capacity and long cycle life zinc ion batteries. *ACS Sustainable Chemistry & Engineering*. **2019**, 7(3), 3364-3371.

67. Marangon, V., Scaduti, E., Vinci, V.F. and Hassoun, J. Scalable Composites Benefiting from Transition-Metal Oxides as Cathode Materials for Efficient Lithium-Sulfur Batteries. *ChemElectroChem*. **2022**, 9(11), e202200374.

68. Zhang, H., Ono, L.K., Tong, G., Liu, Y. and Qi, Y. Long-life lithium-sulfur batteries with high areal capacity based on coaxial CNTs@ TiN-TiO<sub>2</sub> sponge. *Nature Communications*. **2021**, 12(1), 4738.

69. Xue, P., Zhu, K., Gong, W., Pu, J., Li, X., Guo, C., Wu, L., Wang, R., Li, H., Sun, J. and Hong, G., One Stone Two Birds” Design for Dual-Functional TiO<sub>2</sub>-TiN Heterostructures Enabled Dendrite-Free and Kinetics-Enhanced Lithium–Sulfur Batteries. *Advanced Energy Materials*. **2022**, 12(18), 2200308.

70. Wei, X., Luo, Y., Du, X., Wu, L., Liu, G. and Li, J. Porous transition metal oxide scaffold implanted with interpenetrated catalytic network enabling polysulfides restricted and dendrite free Lithium–Sulfur batteries. *Chemical Engineering Journal*. **2023**, 454, 140152.

71. Xu, X., Liu, W., Kim, Y. and Cho, J. Nanostructured transition metal sulfides for lithium ion batteries: progress and challenges. *Nano Today*. **2014**, 9(5), 604-630.

72. Li, J., Xiong, Z., Wu, Y., Li, H., Liu, X., Peng, H., Zheng, Y., Zhang, Q. and Liu, Q. Iron (Fe, Ni, Co)-based transition metal compounds for lithium-sulfur batteries: mechanism, progress and prospects. *Journal of Energy Chemistry*. **2022**.

73. Liang, X., Kwok, C.Y., Lodi-Marzano, F., Pang, Q., Cuisinier, M., Huang, H., Hart, C.J., Houtarde, D., Kaup, K., Sommer, H. and Brezesinski, T. Tuning transition metal oxide–sulfur

interactions for long life lithium sulfur batteries: the “Goldilocks” principle. *Advanced Energy Materials*. **2016**, 6(6), 1501636.

74. He, B., Wang, Z., Li, G., Liu, S. and Gao, X. Perovskite transition metal oxide of nanofibers as catalytic hosts for lithium–sulfur battery. *Journal of Alloys and Compounds*. **2022**, 918, 165660.

75. Wei, X., Luo, Y., Du, X., Wu, L., Liu, G. and Li, J. Porous transition metal oxide scaffold implanted with interpenetrated catalytic network enabling polysulfides restricted and dendrite free Lithium–Sulfur batteries. *Chemical Engineering Journal*. **2023**, 454, 140152.

76. Pu, J., Gong, W., Shen, Z., Wang, L., Yao, Y. and Hong, G. CoNiO<sub>2</sub>/Co<sub>4</sub>N heterostructure nanowires assisted polysulfide reaction kinetics for improved lithium–sulfur batteries. *Advanced Science*. **2022**, 9(4), 2104375.

77. Xu, X., Liu, W., Kim, Y. and Cho, J. Nanostructured transition metal sulfides for lithium ion batteries: progress and challenges. *Nano Today*. **2014**, 9(5), 604-630.

78. Friend, R.H. and Yoffe, A.D. Electronic properties of intercalation complexes of the transition metal dichalcogenides. *Advances in Physics*. **1987**, 36(1), 1-94.

79. Butler, S.Z., Hollen, S.M., Cao, L., Cui, Y., Gupta, J.A., Gutiérrez, H.R., Heinz, T.F., Hong, S.S., Huang, J., Ismach, A.F. and Johnston-Halperin, E. Progress, challenges, and opportunities in two-dimensional materials beyond graphene. *ACS nano*. **2013**, 7(4), 2898-2926.

80. Huisman, R., De Jonge, R., Haas, C. and Jellinek, F. Trigonal-prismatic coordination in solid compounds of transition metals. *Journal of Solid State Chemistry*. **1971**, 3(1), 56-66.

81. Winter, R. and Heitjans, P. Li<sup>+</sup> diffusion and its structural basis in the nanocrystalline and amorphous forms of two-dimensionally ion-conducting Li<sub>x</sub> TiS<sub>2</sub>. *The Journal of Physical Chemistry B*. **2001**, 105(26), 6108-6115.

82. Zhang, Q., Wang, Y., Seh, Z.W., Fu, Z., Zhang, R. and Cui, Y. Understanding the anchoring effect of two-dimensional layered materials for lithium–sulfur batteries. *Nano letters*. **2015**, 15(6), 3780-3786.

83. Su, Y.S. and Manthiram, A. Sulfur/lithium-insertion compound composite cathodes for Li–S batteries. *Journal of Power Sources*. **2014**, 270, 101-105.

84. Xiao, Z., Yang, Z., Zhou, L., Zhang, L. and Wang, R. Highly conductive porous transition metal dichalcogenides via water steam etching for high-performance lithium–sulfur batteries. *ACS Applied Materials & Interfaces*. **2017**, 9(22), 18845-18855.

85. Xu, G., Li, R., Li, M., Zhang, Q., Li, B., Guo, J., Wang, X., Yang, C. and Yu, Y. Rapid internal conversion harvested in Co/Mo dichalcogenides hollow nanocages of polysulfides for stable Lithium-Sulfur batteries. *Chemical Engineering Journal*. **2022**, 434, 134498.
86. Vyskočil, J., Mayorga-Martinez, C.C., Szökölová, K., Dash, A., Gonzalez-Julian, J., Sofer, Z. and Pumera, M. 2D Stacks of MXene  $\text{Ti}_3\text{C}_2$  and 1T-Phase  $\text{WS}_2$  with Enhanced Capacitive Behavior. *ChemElectroChem*. **2019**, 6(15), 3982-3986.
87. Wang, W., Huai, L., Wu, S., Shan, J., Zhu, J., Liu, Z., Yue, L. and Li, Y. Ultrahigh-Volumetric-Energy-Density Lithium-Sulfur Batteries with Lean Electrolyte Enabled by Cobalt-Doped  $\text{MoSe}_2/\text{Ti}_3\text{C}_2\text{T}_x$  MXene Bifunctional Catalyst. *ACS nano*. **2021**, 15(7), 11619-11633.
88. Liang, X., Garsuch, A. and Nazar, L.F. Sulfur cathodes based on conductive MXene nanosheets for high-performance lithium-sulfur batteries. *Angewandte Chemie*. **2015**, 127(13), 3979-3983.
89. Liang, X., Rangom, Y., Kwok, C.Y., Pang, Q. and Nazar, L.F. Interwoven MXene nanosheet/carbon-nanotube composites as Li-S cathode hosts. *Advanced Materials*. **2017**, 29(3), 1603040.
90. Ponnada, S., Babu Gorle, D., Chandra Bose, R.S., Sadat Kiai, M., Devi, M., Venkateswara Raju, C., Baydogan, N., Kar Nanda, K., Marken, F. and Sharma, R.K. Current Insight into 3D Printing in Solid-State Lithium-Ion Batteries: A Perspective. *Batteries & Supercaps*. **2022**, 5(8), e202200223.
91. Ponnada, S., Kiai, M.S., Gorle, D.B., Bose, R.S., Rajagopal, V., Saini, B., Kathiresan, M., Nowduri, A., Singhal, R., Marken, F. and Kulandainathan, M.A. Recent status and challenges in multifunctional electrocatalysis based on 2D MXenes. *Catalysis Science & Technology*. **2022**, 12(14), 4413-4441.
92. Bao, W., Liu, L., Wang, C., Choi, S., Wang, D. and Wang, G. Facile synthesis of crumpled nitrogen-doped mxene nanosheets as a new sulfur host for lithium-sulfur batteries. *Advanced Energy Materials*. **2018**, 8(13), 1702485.
93. Lv, L.P., Guo, C.F., Sun, W. and Wang, Y. Strong surface-bound sulfur in carbon nanotube bridged hierarchical  $\text{Mo}_2\text{C}$ -based MXene nanosheets for lithium-sulfur batteries. *Small*. **2019**, 15(3), 1804338.

94. Shi, N., Xi, B., Feng, Z., Liu, J., Wei, D., Liu, J., Feng, J. and Xiong, S. Strongly coupled W<sub>2</sub>C atomic nanoclusters on N/P-codoped graphene for kinetically enhanced sulfur host. *Advanced Materials Interfaces*. **2019**, 6(9), 1802088.
95. Fan, K. and Huang, H. Two-Dimensional Host Materials for Lithium-Sulfur Batteries: A Review and Perspective. *Energy Storage Materials* (2022).
96. Zhou, W., Cao, G., Yuan, M., Zhong, S., Wang, Y., Liu, X., Cao, D., Peng, W., Liu, J., Wang, G. and Dang, Z.M. Core-shell engineering of conductive fillers toward enhanced dielectric properties: a universal polarization mechanism in polymer conductor composites. *Advanced Materials*. **2023**, 35(2), 2207829.
97. Zong, H., Hu, L., Gong, S., Yu, K. and Zhu, Z. Flower-petal-like Nb<sub>2</sub>C MXene combined with MoS<sub>2</sub> as bifunctional catalysts towards enhanced lithium-sulfur batteries and hydrogen evolution. *Electrochimica Acta*. **2022**, 404, 139781.
98. Sun, J., Sun, Y., Pasta, M., Zhou, G., Li, Y., Liu, W., Xiong, F. and Cui, Y. Entrapment of polysulfides by a black-phosphorus-modified separator for lithium-sulfur batteries. *Advanced materials*. **2016**, 28(44), 9797-9803.
99. Zhang, G., Wang, S., Zeng, X., Li, X., Xiao, L., Chen, K., Lu, Q., Xu, Q., Weng, J. and Xu, J. Holey amorphous FeCoO-coated black phosphorus for robust polysulfide adsorption and catalytic conversion in lithium-sulfur batteries. *Journal of Materials Chemistry A*. **2022**, 10(21), 11676-11683.
100. Li, Z., Zhou, C., Hua, J., Hong, X., Sun, C., Li, H.W., Xu, X. and Mai, L. Engineering oxygen vacancies in a polysulfide-blocking layer with enhanced catalytic ability. *Advanced Materials*. **2020**, 32(10), 1907444.
101. Li, W., Chen, K., Xu, Q., Li, X., Zhang, Q., Weng, J. and Xu, J. Mo<sub>2</sub>C/C Hierarchical Double-Shelled Hollow Spheres as Sulfur Host for Advanced Li-S Batteries. *Angewandte Chemie International Edition*. **2021**, 60(39), 21512-21520.
102. Chen, K., Zhang, G., Xiao, L., Li, P., Li, W., Xu, Q. and Xu, J. Polyaniline Encapsulated Amorphous V<sub>2</sub>O<sub>5</sub> Nanowire-Modified Multi-Functional Separators for Lithium-Sulfur Batteries. *Small Methods*. **2021**, 5(3), 2001056.
103. Zhang, C., Du, R., Biendicho, J.J., Yi, M., Xiao, K., Yang, D., Zhang, T., Wang, X., Arbiol, J., Llorca, J. and Zhou, Y. Tubular CoFeP@ CN as a Mott-Schottky catalyst with multiple



adsorption sites for robust lithium– sulfur batteries. *Advanced Energy Materials*. **2021**, 11(24), 2100432.

104. Jiang, Y., Zhang, D., Li, Y., Yuan, T., Bahlawane, N., Liang, C., Sun, W., Lu, Y. and Yan, M. Amorphous Fe<sub>2</sub>O<sub>3</sub> as a high-capacity, high-rate and long-life anode material for lithium ion batteries. *Nano Energy*. **2014**, 4, 23-30.

105. Shi, L., Li, Y., Zeng, F., Ran, S., Dong, C., Leu, S.Y., Boles, S.T. and Lam, K.H. In situ growth of amorphous Fe<sub>2</sub>O<sub>3</sub> on 3D interconnected nitrogen-doped carbon nanofibers as high-performance anode materials for sodium-ion batteries. *Chemical Engineering Journal*. **2019**, 356, 107-116.

106. Zhang, Q., Xiao, Y., Fu, Y., Li, C., Zhang, X., Yan, J., Liu, J. and Wu, Y. Theoretical prediction of B/Al-doped black phosphorus as potential cathode material in lithium-sulfur batteries. *Applied Surface Science*. **2020**, 512, 145639.

107. Wen, X., Xiang, K., Zhu, Y., Xiao, L., Liao, H., Chen, W., Chen, X. and Chen, H. 3D hierarchical nitrogen-doped graphene/CNTs microspheres as a sulfur host for high-performance lithium-sulfur batteries. *Journal of Alloys and Compounds*. **2020**, 815, 152350.

108. He, B., Wang, Z., Li, G., Liu, S. and Gao, X. Perovskite transition metal oxide of nanofibers as catalytic hosts for lithium–sulfur battery. *Journal of Alloys and Compounds*. **2022**, 918, 165660.

109. Mahankali, K., Thangavel, N.K., Gopchenko, D. and Arava, L.M.R. Atomically engineered transition metal dichalcogenides for liquid polysulfide adsorption and their effective conversion in Li-S batteries. *ACS applied materials & interfaces*. **2020**, 12(24), 27112-27121.

110. Zhong, X., Wang, D., Sheng, J., Han, Z., Sun, C., Tan, J., Gao, R., Lv, W., Xu, X., Wei, G. and Zou, X. Freestanding and sandwich MXene-based cathode with suppressed lithium polysulfides shuttle for flexible lithium–sulfur batteries. *Nano Letters*. **2022**, 22(3), 1207-1216.

111. Huang, Y., Wang, Y. and Fu, Y. A thermoregulating separator based on black phosphorus/MOFs heterostructure for thermo-stable lithium-sulfur batteries. *Chemical Engineering Journal*. **2023**, 454, 140250.

112. Zhang, H. Ultrathin two-dimensional nanomaterials. *ACS nano*. **2015**, 9(10), 9451-9469.

113. Kumar, N.A., Dar, M.A., Gul, R. and Baek, J.B. Graphene and molybdenum disulfide hybrids: synthesis and applications. *Materials Today*. **2015**, 18(5), 286-298.

114. Fan, Y., Yang, Z., Hua, W., Liu, D., Tao, T., Rahman, M.M., Lei, W., Huang, S. and Chen, Y. Functionalized Boron Nitride Nanosheets/Graphene Interlayer for Fast and Long-Life Lithium–Sulfur Batteries. *Advanced Energy Materials*. **2017**, 7(13), 1602380.
115. Deng, D.R., Xue, F., Bai, C.D., Lei, J., Yuan, R., Zheng, M.S. and Dong, Q.F. Enhanced adsorptions to polysulfides on graphene-supported BN nanosheets with excellent Li–S battery performance in a wide temperature range. *ACS nano*. **2018**, 12(11), 11120-11129.
116. Mussa, Y., Bayhan, Z., Althubaiti, N., Arsalan, M. and Alsharaeh, E. Hexagonal boron nitride effect on the performance of graphene-based lithium–sulfur batteries and its stability at elevated temperatures. *Materials Chemistry and Physics*. **2021**, 257, 123807.
117. Curtarolo, S., Hart, G.L., Nardelli, M.B., Mingo, N., Sanvito, S. and Levy, O. The high-throughput highway to computational materials design. *Nature materials*. **2013**, 12(3), 191-201.
118. Curtarolo, S., Hart, G.L., Nardelli, M.B., Mingo, N., Sanvito, S. and Levy, O. The high-throughput highway to computational materials design. *Nature materials*. **2013**, 12(3), 191-201.
119. He, Q., Yu, B., Li, Z. and Zhao, Y. Density functional theory for battery materials. *Energy & Environmental Materials*. **2019**, 2(4), 264-279.
120. Zhang, T., Li, D., Tao, Z. and Chen, J. Understanding electrode materials of rechargeable lithium batteries via DFT calculations. *Progress in Natural Science: Materials International*. **2013**, 23(3), 256-272.
121. Feng, S., Fu, Z.H., Chen, X. and Zhang, Q. A review on theoretical models for lithium–sulfur battery cathodes. *InfoMat*. **2022**, 4(3), e12304.
122. Zhou, F., Cococcioni, M., Marianetti, C.A., Morgan, D. and Ceder, G. First-principles prediction of redox potentials in transition-metal compounds with LDA+U. *Physical Review B*. **2004**, 70(23), 235121.
123. Yu, X., Yang, Y., Si, L., Cai, J., Lu, X. and Sun, Z. V<sub>4</sub>C<sub>3</sub>T<sub>X</sub> MXene: First-principles computational and separator modification study on immobilization and catalytic conversion of polysulfide in Li-S batteries. *Journal of Colloid and Interface Science*. **2022**, 627, 992-1002.
124. Panigrahi, P., Pal, Y., Hussain, T. and Ahuja, R. Application of germanene monolayers as efficient anchoring material to immobilize lithium polysulfides in Li-S batteries. *Applied Surface Science*. **2021**, 558, 149850.

125. Gao, G., Zheng, F., Pan, F. and Wang, L.W. Theoretical investigation of 2D conductive microporous coordination polymers as Li-S battery cathode with ultrahigh energy density. *Advanced Energy Materials*. **2018**, 8(25), 1801823.
126. Bamine, T., Boivin, E., Boucher, F., Messinger, R.J., Salager, E., Deschamps, M., Masquelier, C., Croguennec, L., Ménétrier, M. and Carlier, D. Understanding local defects in Li-ion battery electrodes through combined DFT/NMR studies: Application to LiVPO<sub>4</sub>F. *The Journal of Physical Chemistry C*. **2017**, 121(6), 3219-3227.
127. Maihom, T., Sittiwong, J., Probst, M. and Limtrakul, J. Understanding the interactions between lithium polysulfides and anchoring materials in advanced lithium-sulfur batteries using density functional theory. *Physical Chemistry Chemical Physics*. **2022**, 24(15), 8604-8623.
128. Wang, T., Li, Q., Feng, Q., Miao, Y., Li, T., Qi, J., Wei, F., Meng, Q., Ren, Y., Xiao, B. and Xue, X.. Carbon defects applied to potassium-ion batteries: a density functional theory investigation. *Nanoscale*. **2021**, 13(32), 13719-13734.
129. Yi, Z., Su, F., Huo, L., Cui, G., Zhang, C., Han, P., Dong, N. and Chen, . New insights into Li<sub>2</sub>S<sub>2</sub>/Li<sub>2</sub>S adsorption on the graphene bearing single vacancy: A DFT study. *Applied Surface Science*. **2020**, 503, 144446.
130. Oh, D., Gostovic, D. and Wachsman, E.D. Mechanism of La<sub>0.6</sub>Sr<sub>0.4</sub>Co<sub>0.2</sub>Fe<sub>0.8</sub>O<sub>3</sub> cathode degradation. *Journal of Materials Research*. **2012**, 27(15), 1992-1999.
131. Mansoor, M., Mansoor, M., Mansoor, M., Aksoy, A., Seyhan, S.N., Yıldırım, B., Tahiri, A., Solak, N., Kazmanlı, K., Er, Z. and Czelej, K. Ab-initio calculation of point defect equilibria during heat treatment: Nitrogen, hydrogen, and silicon doped diamond. *Diamond and Related Materials*. **2022**, 126, 109072.
132. Freysoldt, C., Grabowski, B., Hickel, T., Neugebauer, J., Kresse, G., Janotti, A. and Van de Walle, C.G. First-principles calculations for point defects in solids. *Reviews of modern physics*. **2014**, 86(1), 253.
133. Yi, G.S., Sim, E.S. and Chung, Y.C. Effect of lithium-trapping on nitrogen-doped graphene as an anchoring material for lithium-sulfur batteries: a density functional theory study. *Physical Chemistry Chemical Physics*. **2017**, 19(41), 28189-28194.

134. Zeng, Q.W., Hu, R.M., Chen, Z.B. and Shang, J.X. Single-atom Fe and N co-doped graphene for lithium-sulfur batteries: a density functional theory study. *Materials Research Express*. **2019**, 6(9), 095620.
135. Yin, L.C., Liang, J., Zhou, G.M., Li, F., Saito, R. and Cheng, H.M. Understanding the interactions between lithium polysulfides and N-doped graphene using density functional theory calculations. *Nano Energy*. **2016**, 25, 203-210.
136. Mansoor, M., Mansoor, M., Mansoor, M., Er, Z., Czelej, K. and Ürgen, M. Stress-induced changes in phonon frequencies of ZrSiO<sub>4</sub>: Infrared spectroscopy-based pressure sensor. *Solid State Communications*. **2022**, 357, 114983.
137. Qi, Y., Hector, L.G., James, C. and Kim, K.J. Lithium concentration dependent elastic properties of battery electrode materials from first principles calculations. *Journal of The Electrochemical Society*. **2014**, 161(11), F3010.
138. Min, K. High-throughput Ab initio investigation of the elastic properties of inorganic electrolytes for all-solid-state Na-ion batteries. *Journal of The Electrochemical Society*. **2021**, 168(3), 030541.
139. Bahari, Y., Mortazavi, B., Rajabpour, A., Zhuang, X. and Rabczuk, T. Application of two-dimensional materials as anodes for rechargeable metal-ion batteries: A comprehensive perspective from density functional theory simulations. *Energy Storage Materials*. **2021**, 35, 203-282.
140. Chowdhury, E.H., Rahman, M.H., Fatema, S. and Islam, M.M. Investigation of the mechanical properties and fracture mechanisms of graphene/WSe<sub>2</sub> vertical heterostructure: A molecular dynamics study. *Computational Materials Science*. **2021**, 188, 110231.
141. Yang, J., Wang, M.X., Kang, Y.B. and Li, D.J. Influence of bilayer periods on structural and mechanical properties of ZrC/ZrB<sub>2</sub> superlattice coatings. *Applied surface science*. **2007**, 253(12), 5302-5305.
142. Xu, C., Dai, Q., Gaines, L., Hu, M., Tukker, A. and Steubing, B. Future material demand for automotive lithium-based batteries. *Communications Materials*. **2020**, 1(1), 99.
143. Zhang, C.Y., Zhang, C., Pan, J.L., Sun, G.W., Shi, Z., Li, C., Chang, X., Sun, G.Z., Zhou, J.Y. and Cabot, A. Surface strain-enhanced MoS<sub>2</sub> as a high-performance cathode catalyst for lithium-sulfur batteries. *eScience*. **2022**, 2(4), 405-415.

144. Muralidharan, N., Brock, C.N., Cohn, A.P., Schauben, D., Carter, R.E., Oakes, L., Walker, D.G. and Pint, C.L. Tunable mechanochemistry of lithium battery electrodes. *ACS nano*. **2017**, *11*(6), 6243-6251.
145. Zhang, H., Wang, Z., Ren, J., Liu, J. and Li, J. Ultra-fast and accurate binding energy prediction of shuttle effect-suppressive sulfur hosts for lithium-sulfur batteries using machine learning. *Energy Storage Materials*. **2021**, *35*, 88-98.
146. Ponnada, S., Mansoor, M., Aslfattahi, N., Baydogan, N., Naskar, S., Sharma, R.K. and Kiai, M.S. Sustainable Metal-Organic Framework Co-Engineered Glass Fiber Separators for Safer and Longer Cycle Life of Li-S Batteries. *Journal of Alloys and Compounds*. **2023**, 168962.
147. Grixti, S., Mukherjee, S. and Singh, C.V. Two-dimensional boron as an impressive lithium-sulphur battery cathode material. *Energy Storage Materials*. **2018**, *13*, 80-87.
148. Li, F. and Zhao, J. Atomic sulfur anchored on silicene, phosphorene, and borophene for excellent cycle performance of Li-S batteries. *ACS applied materials & interfaces*. **2017**, *9*(49), 42836-42844.
149. Zhou, G., Li, L. and Wang, D.W. X. y. Shan, S. Pei, F. Li, HM Cheng. *Adv. Mater.* **2015**, *27*, 641-647.
150. Khan, S., Ul-Islam, M., Sajjad, M., Hussain, I., Idrees, M., Saeed, M., Imran, M. and Javed, M.S. Nitrogen and sulfur Co-doped two-dimensional highly porous carbon nanosheets for high-performance lithium-sulfur batteries. *Energy & Fuels*. **2022**, *36*(4), 2220-2227.
151. Srinivasan, S., Jothibas, M. and Nesakumar, N. Ameliorating the Energy Storage Performance of Lithium-Sulfur Batteries via Sulfur-Intercalated Titanium Carbide ( $\text{Ti}_3\text{C}_2\text{T}_x$ ) MXene. *Energy & Fuels*. **2022**, *36*(7), 4042-4051.
152. Mukherjee, R., Thomas, A.V., Datta, D., Singh, E., Li, J., Eksik, O., Shenoy, V.B. and Koratkar, N. Defect-induced plating of lithium metal within porous graphene networks. *Nature communications*. **2014**, *5*(1), 3710.
153. Lee, D.K., Ahn, C.W. and Lee, J.W. Electrostatic self-assembly of 2-dimensional MXene-wrapped sulfur composites for enhancing cycle performance of lithium-sulfur batteries. *Electrochimica Acta*. **2022**, *402*, 139539.

